Cannabinoid receptor type 2 promotes kidney fibrosis through orchestrating β-catenin signaling

OPEN

Shan Zhou[1,6], Qinyu Wu[1,6], Xu Lin[2,6], Xian Ling[1], Jinhua Miao[1], Xi Liu[1], Chengxiao Hu[1], Yunfang Zhang[3], Nan Jia[1], Fan Fan Hou[1], Youhua Liu[1,4] and Lili Zhou[1,5]

[1]State Key Laboratory of Organ Failure Research, National Clinical Research Center of Kidney Disease, Division of Nephrology, Nanfang Hospital, Southern Medical University, Guangzhou, China; [2]Department of Nephrology, Affiliated Hospital of Youjiang Medical University for Nationalities, Baise, Guangxi, China; [3]Department of Nephrology, Huadu District People's Hospital, Southern Medical University, Guangzhou, China; [4]Department of Pathology, University of Pittsburgh School of Medicine, Pittsburgh, Pennsylvania, USA; and [5]Bioland Laboratory (Guangzhou Regenerative Medicine and Health, Guangdong Laboratory), Guangzhou, China

The endocannabinoid system has multiple effects. Through interacting with cannabinoid receptor type 1 and type 2, this system can greatly affect disease progression. Previously, we showed that activated cannabinoid receptor type 2 (CB2) mediated kidney fibrosis. However, the underlying mechanisms remain underdetermined. Here, we report that CB2 was upregulated predominantly in kidney tubular epithelial cells in unilateral urinary obstruction and ischemia-reperfusion injury models in mice, and in patients with a variety of kidney diseases. CB2 expression was closely correlated with the progression of kidney fibrosis and accompanied by the activation of β-catenin. Furthermore, CB2 induced the formation of a β-arrestin 1/Src/β-catenin complex, which further triggered the nuclear translocation of β-catenin and caused fibrotic injury. Incubation with XL-001, an inverse agonist to CB2, or knockdown of β-arrestin 1 inhibited CB2-triggered activation of β-catenin and fibrotic injury. Notably, CB2 potentiated Wnt1-induced β-arrestin 1/β-catenin activation and augmented the pathogenesis of kidney fibrosis in mice with unilateral ischemia-reperfusion injury or folic acid-induced nephropathy. Knockdown of β-arrestin 1 inhibited the CB2 agonist AM1241-induced β-catenin activation and kidney fibrosis. By promoter sequence analysis, putative transcription factor binding sites for T-cell factor/lymphoid enhancer factor were found in the promoter regions of the CB2 gene regardless of the species. Overexpression of β-catenin induced the binding of T-cell factor/lymphoid enhancer factor-1 to these sites, promoted the expression of CB2, β-arrestin 1, and the proto-oncogene Src, and triggered their accumulation. Thus, the CB2/β-catenin pathway appears to create a reciprocal activation feedback loop that plays a central role in the pathogenesis of kidney fibrosis.

Correspondence: *Lili Zhou, Division of Nephrology, Nanfang Hospital, 1838 North Guangzhou Avenue, Guangzhou 510515, China. E-mail: jinli730@smu.edu.cn*

[6]SZ, QW, and XL contributed equally to this work.

Received 8 October 2019; revised 27 August 2020; accepted 3 September 2020; published online 2 November 2020

Kidney International (2021) **99,** 364–381; https://doi.org/10.1016/j.kint.2020.09.025

KEYWORDS: β-arrestin 1; β-catenin; CB2; renal fibrosis; tubular cells

Translational Statement

Cannabinoid receptors are involved in tissue fibrosis. Although cannabinoid receptor type 1 activation has been reported to mediate renal fibrosis, the role of cannabinoid receptor type 2 (CB2) remains to be demonstrated in detail. This study provides evidence for the detrimental role of CB2 in the pathogenesis of renal fibrosis. The findings highlight a novel CB2/β-catenin pathway that promotes renal fibrosis. Blockade of CB2 is a potential therapeutic intervention to prevent renal fibrosis in a variety of nephropathies. The findings also provide health warnings to the fast-growing group of exocannabinoid consumers, for both recreational and medicinal purposes.

The endocannabinoid system plays a critical role in cardiovascular, neurodegenerative, and metabolic diseases.[1–4] Through interacting with cannabinoid receptors type 1 (CB1) and type 2 (CB2),[5] the endocannabinoid system could also affect the prognosis of kidney diseases.[6] CB1 plays a detrimental role in renal fibrosis.[7–9] However, the role of CB2 in renal fibrosis remains elusive.

CB2 was previously reported to be involved in the immune system.[10] Recently, CB2 was found to be expressed in kidneys.[3,11–13] In early diabetic nephropathy and podocytes, CB2 plays a protective role in cellular integrity.[3] However, in fibrotic injury, CB2 is upregulated in tubular cells and involved in fibrogenic responses, as reported in our previous work.[11] CB2 is also expressed in interstitial fibroblasts and macrophages and mediates their activation.[11] Of note, the levels of 2-arachidonoylglyceril (2-AG), the main endogenous ligand of CB2, are also increased in obstructive kidneys.[7] Although a previous study pointed out that the activation

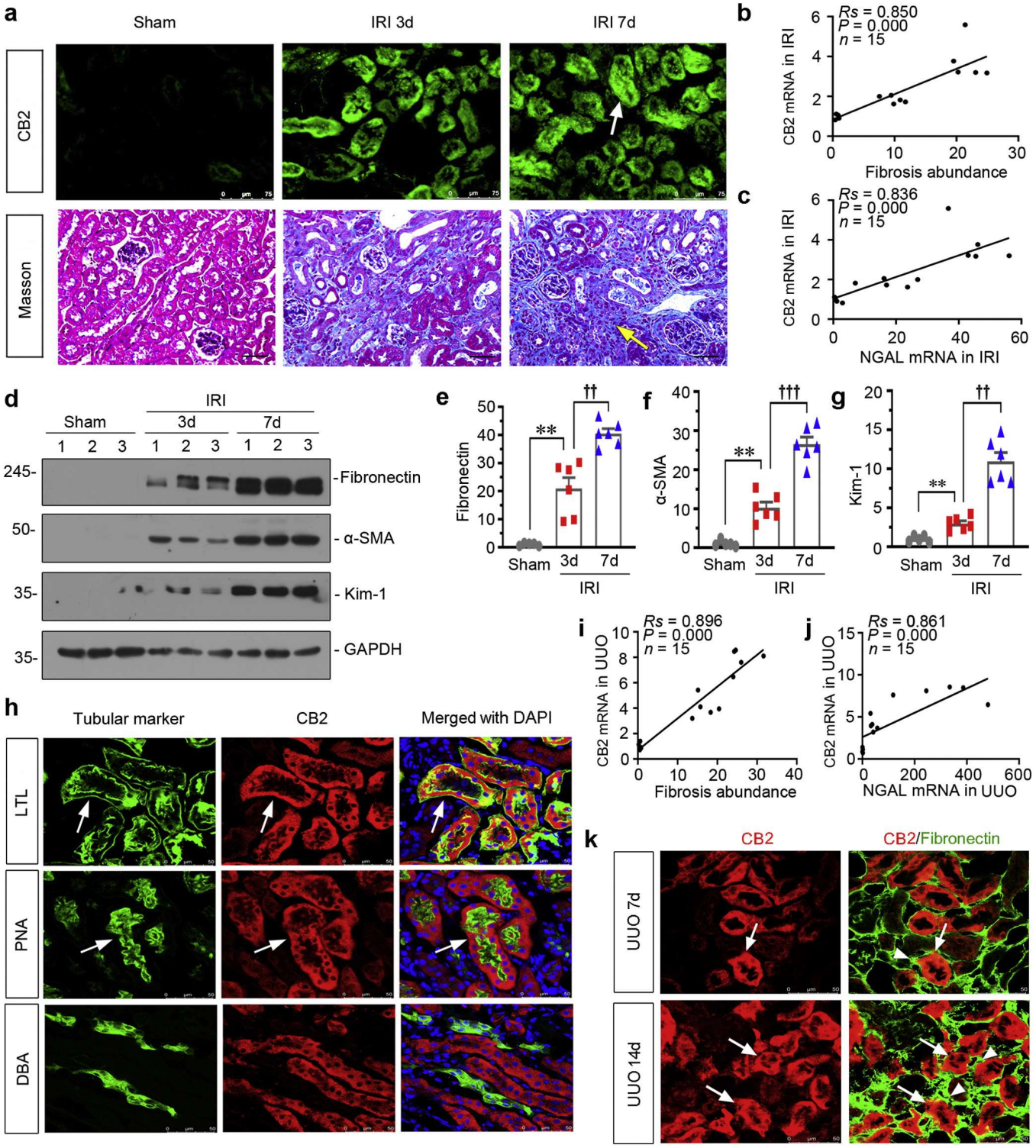

Figure 1 | Cannabinoid receptor type 2 (CB2) is time-dependently induced in injured kidneys and associated with fibrogenesis. (**a**) Representative micrographs showing CB2 expression and collagen deposition in kidneys after ischemia-reperfusion injury (IRI). IRI surgery was performed in mice, and mice were sacrificed at the indicated time points. Cryosections were subjected to fluorescence *in situ* hybridization (FISH) staining for CB2 (top), and paraffin sections were subjected to Masson's trichrome staining for collagen deposition (bottom). Arrows indicate positive staining. For CB2 FISH staining, bar = 75 μm; for Masson's trichrome staining, bar = 50 μm. (**b**,**c**) Linear regression showing renal CB2 is positively correlated with the extent of fibrosis or neutrophil gelatinase–associated lipocalin (NGAL) expression in the IRI mouse model. Mice were sacrificed at 3 or 7 days after IRI. Renal mRNA levels of CB2 and NGAL were assessed by quantitative polymerase chain reaction. The degree of kidney fibrosis was analyzed by quantification of Masson's trichrome staining. The Spearman correlation coefficient (*Rs*) and *P* value are shown. (**d**–**g**) Representative Western blot and quantitative data showing renal expression of fibronectin, α–smooth muscle actin (SMA), and kidney injury molecule-1 (Kim-1) at indicated time points after IRI. Numbers (1–3) indicate each individual animal in a given group. $^{**}P < 0.01$ versus the sham control group; $\dagger\dagger P < 0.01$; $\dagger\dagger\dagger P < 0.001$ versus the IRI 3d group (n = 5–6). (Continued)

of CB2 by agonists protects against renal fibrosis,[7] a genetic CB2 deficiency and a compound (XL-001) with high selectivity to CB2 over CB1 reduce renal fibrotic lesions,[11] which demonstrates the deleterious role of CB2 in renal fibrosis. Consistently, evidence derived from studies in other tissues has shown that genetic CB2 deficiency reduces collagen accumulation and inflammatory cell infiltration.[14,15] However, how CB2 exactly triggers renal fibrosis is poorly understood.

G protein–coupled receptors (GPCRs), the largest family of cell-surface receptors, play a fundamental role in angiogenesis, hormone release, neurotransmission, and immune surveillance.[16,17] Overactivated GPCRs are linked to metastasis,[18] cardiovascular diseases,[19,20] and neurodegenerative disorders.[21] Some GPCRs, such as angiotensin II type I receptor (AT1R), endothelin receptor type A (ETAR), and C-X-C chemokine receptor type 4 (CXCR4), also play central roles in kidney diseases.[22–24] The activation of GPCRs mainly relies on the G protein–mediated receptor phosphorylation and recruitment of β-arrestins, the scaffold proteins for receptor desensitization, internalization, and trafficking.[25,26] Among 4 highly homologous isoforms in mammals,[26] β-arrestin 1 is most responsible for signal transduction of extracellular signal-regulated protein kinase (ERK1/2) and the SRC proto-oncogene (Src).[25,27,28] Src is a member of the nonreceptor tyrosine kinase family. Src phosphorylation (on Tyr^{416}) leads to the activation of downstream pathways.[29] Notably, CB2 belongs to the family of GPCRs, and it is activated by the recruitment of β-arrestins.[27] However, their roles in renal tubular cell injury remain poorly understood.

As a developmental pathway, β-catenin is silent in adult kidneys, but it is reactivated in a variety of nephropathies.[30,31] Through binding to the T-cell factor/lymphoid enhancer binding factor to transactivate its target genes, β-catenin signaling is strongly associated with renal tubular cell atrophy, senescence, and fibrotic injury.[32–34] It is notable that the phosphorylation of tyrosine or dephosphorylation of serine/threonine leads to the activation of β-catenin,[35] suggesting a potential correlation between Src and β-catenin activation. However, the precise relationships between them are undetermined.

In this study, we examined the role of β-catenin in CB2 signaling in chronic kidney disease (CKD)–associated tubular cell injury *in vivo* and *in vitro* and identified the vicious cycle in the CB2/β-catenin pathway.

RESULTS

CB2 is time-dependently induced in injured kidneys and is associated with fibrogenesis

CB2 expression was assessed by *in situ* hybridization. As shown in Figure 1a, CB2 expression was time-dependently upregulated from 3 days after severe ischemia-reperfusion injury (IRI), a key time point at which acute kidney injury would progress into CKD when β-catenin is continually activated,[36] and predominantly located in renal tubular cells. Collagen deposition was examined by Masson's trichrome staining. The extent of collagen deposition was increased with the progression of disease and was positively correlated with the mRNA level of CB2 (Figure 1a and b). Furthermore, the CB2 mRNA level was also positively correlated with the expression of neutrophil gelatinase–associated lipocalin, a marker of tubular injury (Figure 1c). We then analyzed the expression of fibronectin and α-smooth muscle actin (α-SMA), which are fibrogenesis-related factors.[11] Their expression levels were time-dependently increased (Figure 1d–f). In addition, the expression of kidney injury molecule-1 (Kim-1), a marker of tubular damage, was upregulated in a time-dependent fashion (Figure 1d and g). We then performed costaining for CB2 with different segment-specific tubular cell markers—lotus tetragonolobus lectin, a marker of proximal tubules; peanut agglutinin, a marker of distal convoluted tubules; and dolichos biflorus agglutinin, a marker of collecting duct epithelium. CB2 was mainly colocalized with proximal and distal tubular segments, whereas it was barely detectable in the collecting duct (Figure 1h). We next assessed the correlation of CB2 with tubular injury and fibrosis in unilateral ureteral obstruction (UUO) mice. As shown in Figure 1i and j, the mRNA level of CB2 was positively correlated with renal fibrosis and neutrophil gelatinase–associated lipocalin expression. Furthermore, costaining for CB2 and fibronectin in UUO mice also confirmed that CB2 overexpression is related to the progression of fibrogenesis (Figure 1k). The specificity of the *in situ* hybridization staining for CB2 in mouse IRI and UUO models was also checked with a primary CB2 antibody, and verified in CB2 knockout mice as well using a scramble probe as a negative control (Supplementary Figure S1).

Upregulation of CB2 is concomitant with the activation of β-catenin signaling in IRI kidneys

As β-catenin dictates the progression of acute kidney injury to CKD and plays a role in renal fibrosis,[33,36] we further

Figure 1 | (Continued) (**h**) Colocalization of CB2 and various segment-specific tubular markers in kidneys from IRI mice. Frozen kidney sections were harvested 7 days after IRI, and stained for CB2 (red) using FISH, as well various segment-specific tubular markers (green) by immunofluorescence. The following segment-specific tubular markers were used: proximal tubule, lotus tetragonolobus lectin (LTL); distal tubule, peanut agglutinin (PNA); and collecting duct, dolichos biflorus agglutinin (DBA). Arrows indicate positive tubules with colocalization of CB2 and specific tubular markers. Bar = 50 μm. (**i,j**) Linear regression showing the positive correlations between CB2 mRNA level and fibrosis score or NGAL mRNA in kidneys after unilateral ureteral obstruction (UUO). Mice were sacrificed at 7 and 14 days. Renal mRNA levels of CB2 and NGAL, and the degree of fibrosis, were quantified, and the correlation was assessed. The *Rs* and *P* values are shown. (**k**) Representative micrographs showing the expression of CB2 and fibronectin in UUO mice. Frozen kidney sections from mice 7 or 14 days after UUO were analyzed by CB2 FISH and costained with an antibody against fibronectin by immunofluorescence. Arrows indicate CB2-positive tubules. Arrowheads indicate positive staining of fibronectin. Bar = 50 μm. DAPI, 4′,6-diamidino-2-phenylindole; GAPDH, glyceraldehyde 3-phosphate dehydrogenase. To optimize viewing of this image, please see the online version of this article at www.kidney-international.org.

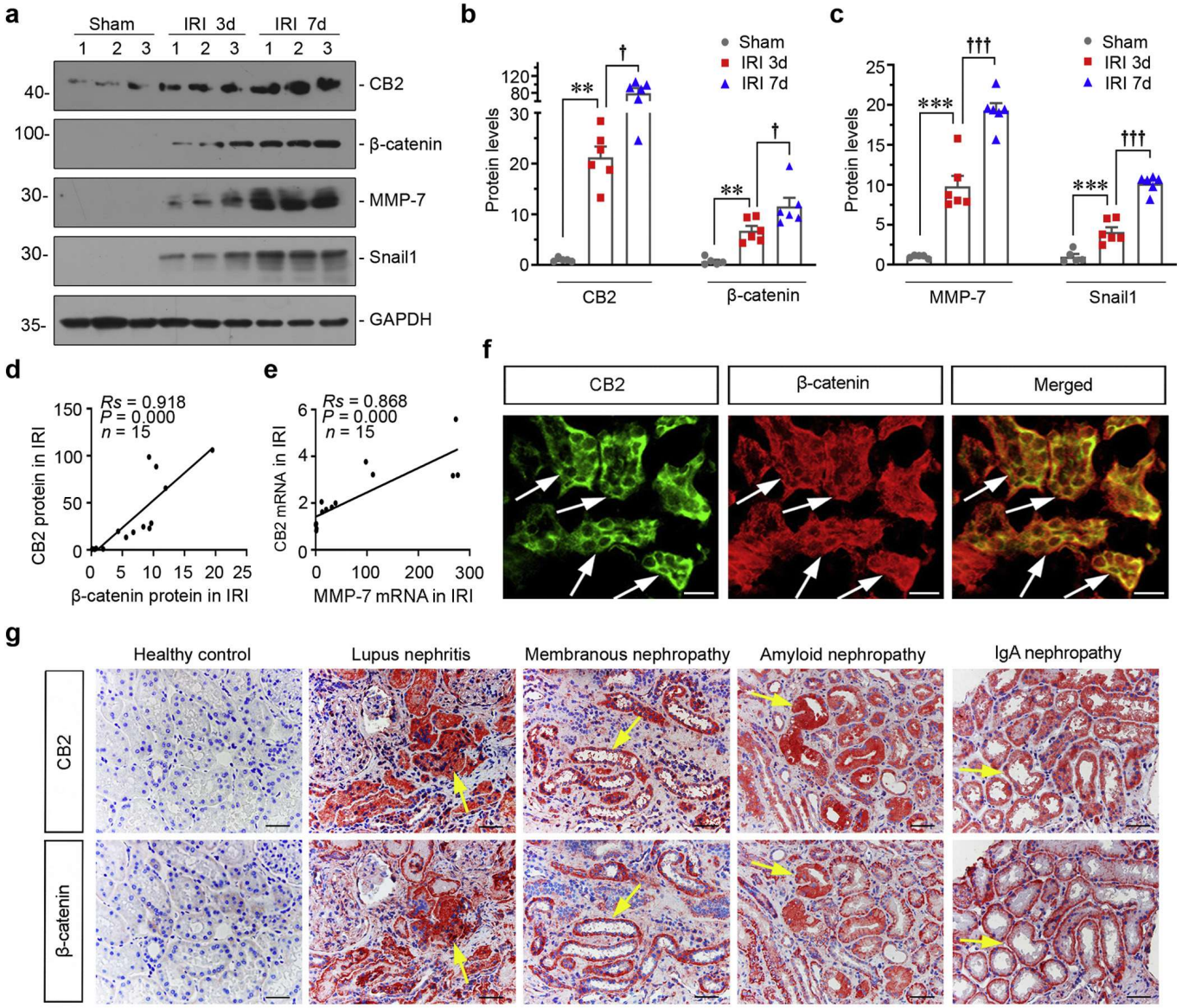

Figure 2| Upregulation of cannabinoid receptor type 2 (CB2) is concomitant with the activation of β-catenin signaling in ischemia-reperfusion injury (IRI) kidneys and human biopsies. (**a–c**) Representative Western blot and quantitative data showing renal expression of CB2, β-catenin, matrix metalloproteinase (MMP)-7, and Snail1 in IRI mice. Numbers (1–3) indicate each individual animal in a given group. $^{**}P < 0.01$; $^{***}P < 0.001$ versus the sham control group; †$P < 0.05$; †††$P < 0.001$ versus the IRI 3d group (n = 5–6). (**d**,**e**) Linear regression showing renal CB2 is positively correlated with (**d**) β-catenin and (**e**) MMP-7 expression in IRI mice. The correlation analysis of renal CB2 and β-catenin protein levels was performed. Renal mRNA levels of CB2 and MMP-7 were assessed by quantitative polymerase chain reaction, followed by the assessment of correlation. The Spearman correlation coefficients (*Rs*) and *P* values are shown. (**f**) Representative images showing colocalization of CB2 and β-catenin in IRI-affected tubules. Frozen kidney sections from mice 7 days after IRI were subjected to fluorescence *in situ* hybridization staining of CB2 (green) and immunofluorescence staining of β-catenin (red). Arrows indicate positive staining. Bar = 20 μm. (**g**) Representative micrographs showing colocalization of CB2 and β-catenin in patients with a variety of nephropathies. Sequential paraffin-embedded kidney sections were immunostained with an antibody against CB2 or β-catenin. Yellow arrows indicate positive staining. Bar = 50 μm. GAPDH, glyceraldehyde 3-phosphate dehydrogenase. To optimize viewing of this image, please see the online version of this article at www.kidney-international.org.

analyzed the correlation between CB2 and β-catenin signaling. Along with CB2, we assessed the expression of β-catenin and its downstream targets matrix metalloproteinase (MMP)-7 and Snail1, the 2 mediators of renal fibrosis.[31,33,34] They were time-dependently upregulated in IRI mice (Figure 2a–c). Furthermore, the expression of CB2 was positively correlated with β-catenin and its downstream target MMP-7 (Figure 2d and e). We then performed costaining for β-catenin and CB2. CB2 was predominantly localized in the renal tubular epithelium with positive expression of β-catenin (Figure 2f). We also examined CB2 and β-catenin expression using kidney sequential sections of humans with lupus nephritis, membranous nephropathy, amyloid nephropathy, and immunoglobulin A nephropathy (IgAN). As shown in

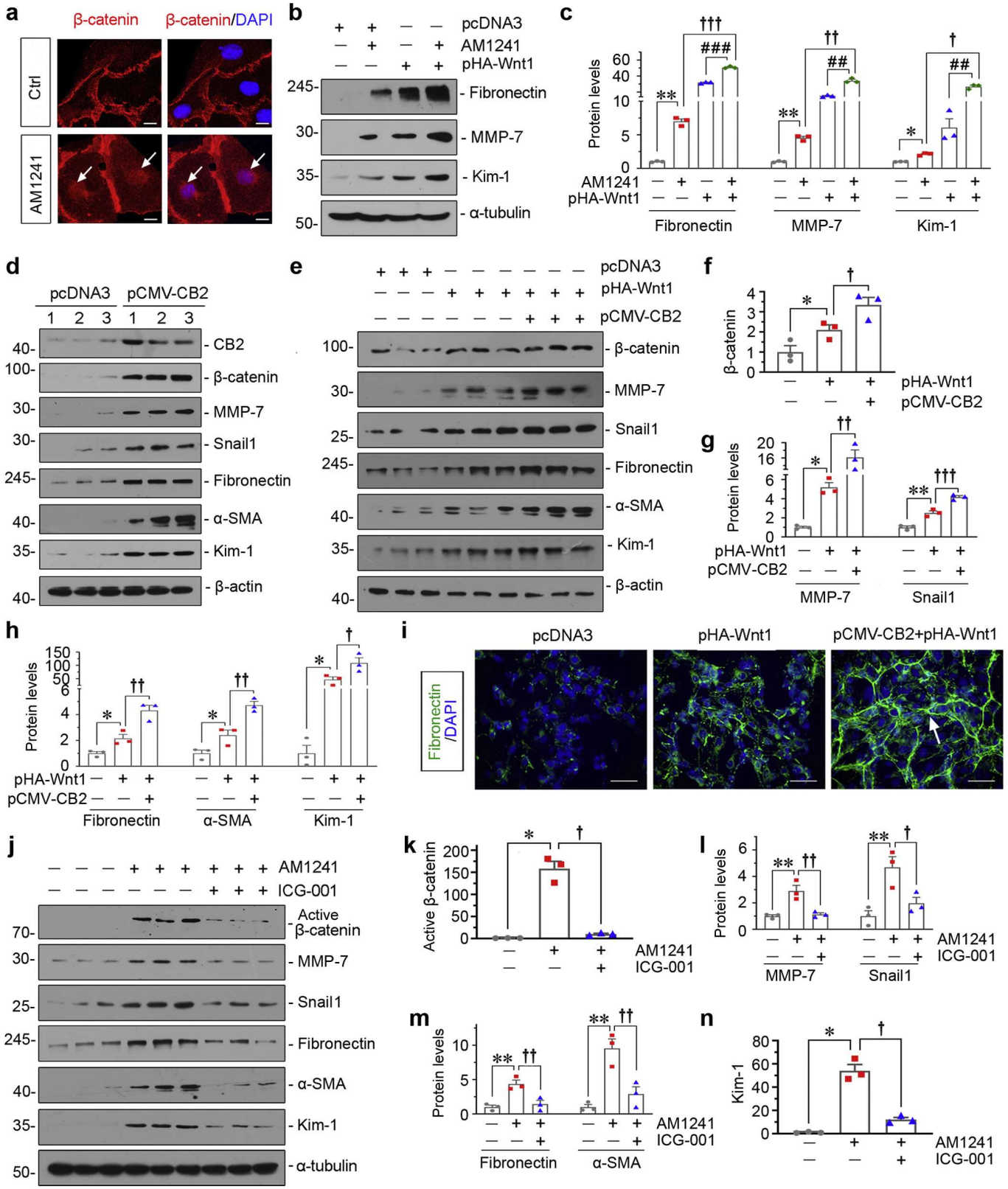

Figure 3 | Cannabinoid receptor type 2 (CB2) induces fibrotic lesions through activation of β-catenin *in vitro*. (**a**) Representative immunofluorescence micrographs showing nuclear translocation of β-catenin in human kidney proximal tubular (HKC-8) cells treated with aminoalkylindole (AM)1241 (10 μM) for 12 hours. Arrows indicate positive staining. Bar = 10 μm. (**b**,**c**) Representative Western blot and quantitative data showing the expression of fibronectin, matrix metalloproteinase (MMP)-7, and kidney injury molecule-1 (Kim-1). HKC-8 cells were transfected with Wnt1 expression plasmid (pHA-Wnt1), and/or treated with AM1241 for 24 hours. Whole-cell lysates were analyzed by Western blot. $^{*}P < 0.05$; $^{**}P < 0.01$ versus the controls; $^{\dagger}P < 0.05$; $^{\dagger\dagger}P < 0.01$; $^{\dagger\dagger\dagger}P < 0.001$ versus the AM1241 group alone; (continued)

Figure 2g, compared with the weak signal in healthy kidneys, CB2 expression was greatly enhanced in all of the biopsy specimens from patients and largely colocalized with β-catenin in tubular cells, although some interstitial fibroblasts and leucocytes were also stained positively. The specific staining of CB2 was verified in CB2 knockout mice (Supplementary Figure S1).

CB2 induces fibrotic lesions through activation of β-catenin in cultured tubular cells

Human kidney proximal tubular (HKC)-8 cells, a human proximal tubular epithelial cell line, were treated with aminoalkylindole (AM)1241, a CB2-specific agonist.[11] As shown in Figure 3a, AM1241 induced the nuclear translocation of β-catenin, an active form of β-catenin.[31] Ectopic expression of Wnt1 significantly induced the upregulation of fibronectin, MMP-7, and Kim-1, which were further upregulated after cotreatment with AM1241 (Figure 3b and c). Overexpression of CB2 induced the upregulation of β-catenin and its targets MMP-7 and Snail1, and triggered the increase in the fibronectin, α-SMA, and Kim-1 levels (Figure 3d; Supplementary Figure S2). Furthermore, Wnt1 induced increases of the above-mentioned factors were further stimulated by cotransfection with a CB2 expression plasmid (Figure 3e–h). A similar result was observed when fibronectin was visualized by immunostaining (Figure 3i). HKC-8 cells were treated with AM1241 after pretreatment with ICG-001, a small molecule that antagonizes β-catenin–mediated gene transcription.[30,32] As shown in Figure 3j–n, ICG-001 nearly completely blocked AM1241-induced upregulation of those proteins. These data suggest that β-catenin plays a critical role in mediating CB2 signaling.

β-arrestin 1/Src complex mediates CB2-induced activation of β-catenin signaling

HKC-8 cells were treated with AM1241 in the absence or presence of XL-001, a selective novel inverse agonist of CB2 established in our group.[11] As shown in Figure 4a, AM1241 triggered the recruitment of β-arrestin 1 and Src to CB2. Cotreatment with XL-001 blocked the formation of a CB2/β-arrestin 1/Src complex. Furthermore, AM1241 induced the binding of β-arrestin 1 with β-catenin, which led to its phosphorylation at tyrosine sites, an active form of β-catenin (Figure 4b). Interestingly, AM1241 induced nuclear translocation of both β-catenin and β-arrestin 1 (Figure 4c). This finding is consistent with a previous report showing that β-arrestin 1 serves as a scaffold protein to initiate β-catenin signaling activation in cancer.[37] We then examined their levels in the cytosolic and nuclear fractions. Despite the upregulation in cytosol, β-arrestin 1 and β-catenin were mainly distributed in the nucleus after treatment with AM1241. Coincubation of XL-001 significantly inhibited both the cytosolic and nuclear upregulation of β-arrestin 1 and β-catenin (Figure 4d–g). Ectopic expression of CB2 induced the upregulation of the transcriptional activity of β-catenin, and it was further elevated by coexpression with β-arrestin 1; however, knockdown of β-arrestin 1 significantly reduced CB2-induced β-catenin transcriptional levels (Figure 4h), and greatly inhibited CB2-induced upregulation of active β-catenin, MMP-7, Snail1, fibronectin, α-SMA, and Kim-1 (Figure 4i–o). Similar results were obtained when fibronectin expression was assessed by immunostaining (Figure 4p). These data suggest an important role of β-arrestin 1/Src in CB2-induced β-catenin activation.

Exogenous CB2 and Wnt1 synergistically induce renal fibrosis in unilateral IRI (UIRI) mice

As shown in Figure 5a, at 4 days after surgery, UIRI mice were injected with various expression plasmids—empty vector (pcDNA3), Wnt1 expression vector (pHA-Wnt1), or both CB2 and Wnt1 expression vectors (pCMV-CB2 + pHA-Wnt1) through hydrodynamic-based gene delivery, an approach that is commonly used to ectopically express proteins in liver and kidneys.[30,31] CB2 expression was characterized by quantitative polymerase chain reaction (PCR) and *in situ* hybridization (Figure 5b and c). We then analyzed renal fibrotic lesions. As shown in Figure 5c and d, ectopic expression of CB2 or Wnt1 increased matrix deposition in UIRI kidneys, whereas coexpression of CB2 and Wnt1 resulted in more substantial kidney lesions and fibrosis, suggesting that CB2 and Wnt1 cooperatively promote the development of kidney fibrosis. Similarly, coexpression of CB2 and Wnt1 induced an increase in serum creatinine in CB2- or Wnt1-overexpressing mice (Figure 5e). As shown in Figure 5f–h, ectopic expression of CB2 or Wnt1 induced the upregulation of fibronectin and α-SMA; however, coexpression of CB2 and Wnt1 further elevated these effects. Similar results were obtained when fibronectin and collagen I were assessed by immunostaining (Figure 5i).

Figure 3 | (continued) $^{\#\#}P < 0.01$; $^{\#\#\#}P < 0.001$ versus the pHA-Wnt1 group alone (n = 3). (**d**) Representative Western blot showing that CB2 triggered the upregulation of β-catenin, MMP-7, Snail1, fibronectin, α–smooth muscle actin (SMA), and Kim-1. HKC-8 cells were transfected with pCMV-CB2 plasmid for 24 hours. (**e–h**) Representative Western blot and quantitative data showing that CB2 increased Wnt1-induced β-catenin, MMP-7, Snail1, fibronectin, α-SMA, and Kim-1 expression in HKC-8 cells. HKC-8 cells were transfected with pHA-Wnt1 plasmid with or without pCMV-CB2 plasmid for 24 hours. $^{*}P < 0.05$; $^{**}P < 0.01$ versus the controls; $^{\dagger}P < 0.05$; $^{\dagger\dagger}P < 0.01$; $^{\dagger\dagger\dagger}P < 0.001$ versus the pHA-Wnt1 group alone (n = 3). (**i**) Representative micrographs showing the immunofluorescence staining of fibronectin. HKC-8 cells were transfected with pHA-Wnt1 plasmid with or without pCMV-CB2 plasmid for 24 hours. The arrow indicates positive staining. Bar = 50 μm. (**j–n**) Representative Western blot and quantitative data showing the expression of active-β-catenin, MMP-7, Snail1, fibronectin, α-SMA, and Kim-1. HKC-8 cells were pretreated with ICG-001 (10 μM) for 1 hour, followed by the stimulation of AM1241 (10 μM) for 24 hours. $^{*}P < 0.05$; $^{**}P < 0.01$ versus the controls; $^{\dagger}P < 0.05$; $^{\dagger\dagger}P < 0.01$ versus the AM1241 group alone (n = 3). Ctrl, control; DAPI, 4′,6-diamidino-2-phenylindole. To optimize viewing of this image, please see the online version of this article at www.kidney-international.org.

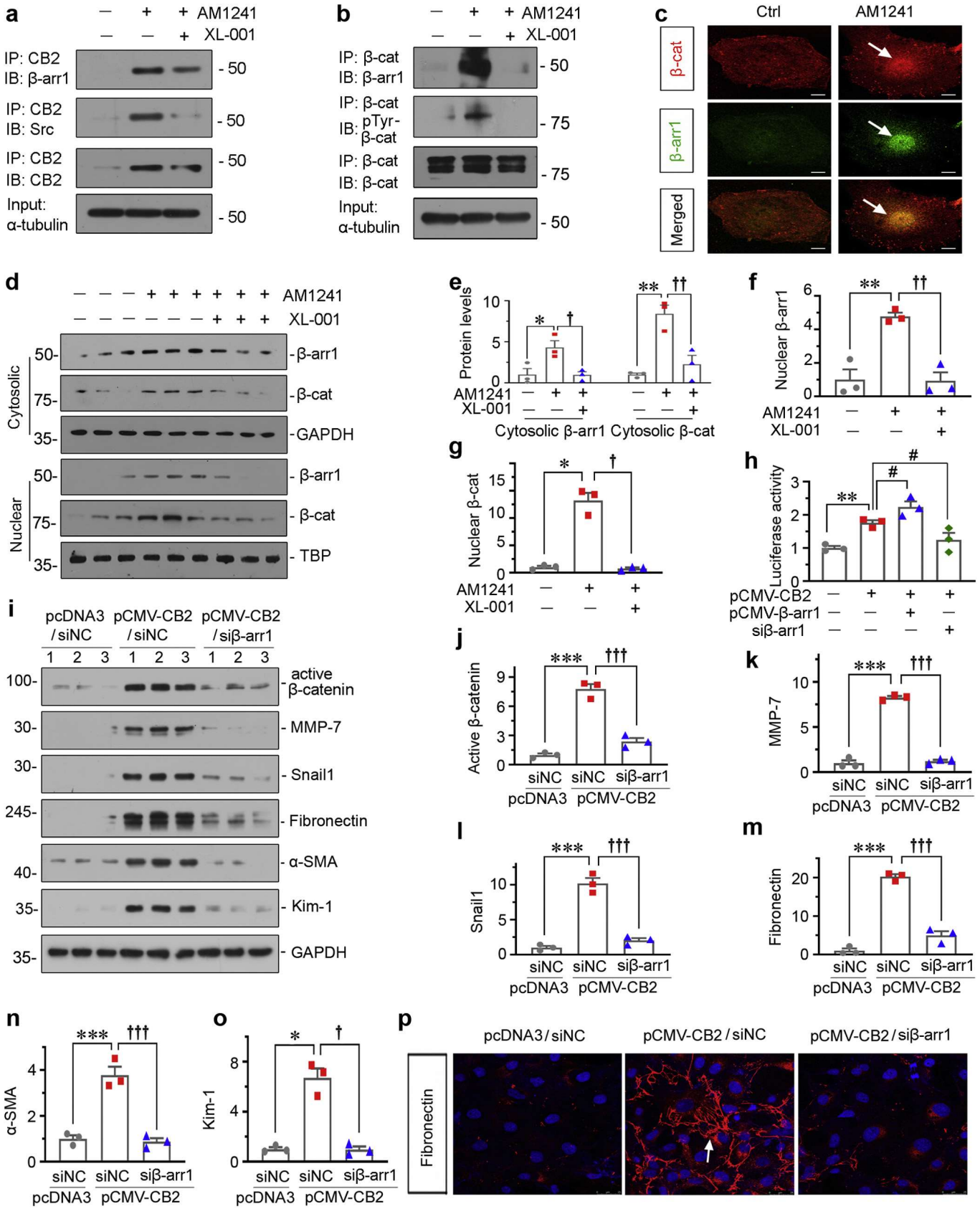

Figure 4| The β-arrestin 1 (β-arr1)/SRC proto-oncogene (Src) complex mediates cannabinoid receptor type 2 (CB2)-induced activation of β-catenin (β-cat) signaling. (**a**) Representative graphs show the binding of CB2 with β-arr1 or Src. Human kidney proximal tubular (HKC-8) cells were treated with aminoalkylindole (AM1241; 10 μM) alone, or cotreated with XL-001 (10 μM) for 24 hours. Whole-cell lysates were immunoprecipitated with an antibody against CB2 and blotted with antibodies against β-arr1 and Src. (Continued)

CB2 amplifies Wnt signaling by promoting the β-arrestin 1/Src/β-catenin pathway

As shown in Figure 6a–c, ectopic expression of CB2 or Wnt1 induced the upregulation of β-arrestin 1 and phospho-Src (Tyr^{416}), an active form of Src.[29] The expression levels of β-arrestin 1 and phospho-Src (Tyr^{416}) were further enhanced by coexpression of CB2 and Wnt1. We then performed costaining for CB2 with β-catenin by *in situ* hybridization and immunofluorescence in UIRI mice with coexpression of CB2 and Wnt1. Nearly all CB2-positive tubular cells expressed β-catenin, implicating the potential role of β-catenin in the CB2 pathway (Figure 6d). We next tested the expression of β-arrestin 1 and active β-catenin by immunofluorescence staining. As shown in Figure 6e, CB2 cooperated with Wnt1 to increase their expression. Furthermore, in UIRI mice, CB2- or Wnt1-induced activation of β-catenin and its targets MMP-7 and Snail1 were further increased by coexpression with each other (Figure 6f–i). The similar expression pattern of Kim-1, as assessed by immunohistochemistry and Western blot analysis, also demonstrated that CB2 had a synergistically stimulatory effect on Wnt1-induced tubular injury (Figure 6e, f, and j).

Exogenous CB2 and Wnt1 synergistically induce β-catenin signaling and renal fibrosis in folic acid–induced nephropathy

The detailed experimental design is shown in Figure 7a. As shown in Figure 7b and c, in folic acid–induced kidneys, ectopic expression of CB2 or Wnt1 induced the upregulation of CB2, and CB2 levels were further elevated by coexpression of CB2 and Wnt1. We then examined the expression of β-arrestin 1 and phospho-Src (Tyr^{416}). As shown in Figure 7d–g, exogenous CB2 and Wnt1 synergistically increased expression of both β-arrestin 1 and phospho-Src. Furthermore, immunostaining of active β-catenin showed that CB2 or Wnt1 increased the activation of β-catenin, and they had a cooperative effect (Figure 7d). Similar results were obtained when the expression of active β-catenin and its downstream targets MMP-7 and Snail1 were assessed by Western blot (Figure 7h–k). The expressional levels of Kim-1, fibronectin, and α-SMA, were upregulated by ectopic expression of CB2 or Wnt1 and further elevated by their coexpression (Figures 7h and l, and 8a–c). Similar results were obtained when fibronectin, collagen I, Kim-1, and Masson's trichrome staining were assessed (Figure 8d). These results further suggest that CB2 plays an active role in the β-arrestin 1/Src–induced β-catenin pathway.

Knockdown of β-arrestin 1 ameliorates β-catenin signaling and renal fibrosis in AM1241-induced UIRI mice

We then examined the role of short hairpin RNA–mediated *in vivo* silencing of β-arrestin 1 in UIRI mice injected with AM1241 (Figure 9a). The silencing efficacy of β-arrestin 1 was confirmed by quantitative real-time PCR (Figure 9b). Administration of AM1241 further increased serum creatinine and blood urea nitrogen levels; however, knockdown of β-arrestin 1 significantly inhibited these increases even in UIRI mice after AM1241 administration (Figure 9c and d). The quantification of periodic acid–Schiff staining (Supplementary Figure S3) showed that knockdown of β-arrestin 1 greatly protected against AM1241-induced tubular injury (Figure 9e). The immunostaining results showed that knockdown of β-arrestin 1 inhibited AM1241-upregulated active β-catenin expression (Figure 9f). Furthermore, the staining results of fibronectin, collagen I, and Kim-1 further confirmed the protective role of interference with β-arrestin 1 in kidney fibrogenesis (Figure 9g). Similar results were observed when the expression of active β-catenin, MMP-7, Snail1, fibronectin, α-SMA, or Kim-1 was assessed by Western blot analysis (Figure 9h–n). Interestingly, we observed that β-arrestin 1 knockdown inhibited CB2 expression, suggesting an activation loop among CB2, β-arrestin 1, and β-catenin (Figure 9h and o). Masson's trichrome staining and quantification of the fibrotic area further demonstrated β-arrestin 1 silencing potently inhibited AM1241-accelerated renal fibrosis (Figure 9g and p).

CB2 is a downstream target of β-catenin and facilitates an activation loop with β-catenin

There were multiple copies of perfect putative T-cell factor / lymphoid enhancer binding factor binding sites in the promoter regions of both human and mouse CB2 genes (Figure 10a). HKC-8 cells were transfected with N-terminally truncated, FLAG-tagged, constitutively activated

Figure 4 | (Continued) (**b**) Representative graphs also show the binding of β-catenin (cat) with β-arr1, and the phosphorylation of β-cat (Tyr^{333}). (**c**) Representative micrographs show the colocalization of β-cat (red) and β-arr1 (green). HKC-8 cells were stimulated with AM1241 for 12 hours. Arrows indicate positive staining. Bar = 10 μm. (**d–g**) Representative Western blot showing the expression of β-arr1 and β-cat in cytosolic and nuclear fractions. HKC-8 cells were treated with AM1241 (10 μM) alone or cotreated with XL-001 (10 μM) for 12 hours. The expression of cytosolic and nuclear proteins was normalized to glyceraldehyde 3-phosphate dehydrogenase (GAPDH) and TATA binding protein (TBP), respectively. $^{*}P < 0.05$; $^{**}P < 0.01$ versus the controls; $^{\dagger}P < 0.05$; $^{\dagger\dagger}P < 0.01$ versus the AM1241 group alone (n = 3). (**h**) The TOP-Flash reporter luciferase assay results in different groups, as indicated. 293-T cells were transfected with pCMV-CB2 plasmid alone, or cotransfected with β-arr1 overexpression plasmid (pCMV-β-arr1) or small interfering (si)RNA. TOP-Flash reporter luciferase activities were measured. The relative luciferase activity (fold change) is reported. $^{**}P < 0.01$ versus the controls; $^{\#}P < 0.05$ versus the pCMV-CB2 group alone (n = 3). (**i–o**) Representative Western blot and quantitative data showing the expression of active β-catenin, matrix metalloproteinase (MMP)-7, Snail1, fibronectin, α–smooth muscle actin (SMA), and kidney injury molecule-1 (Kim-1). HKC-8 cells were transfected with pCMV-CB2 plasmid in the absence or presence of β-arr1 siRNA for 24 hours. $^{*}P < 0.05$; $^{***}P < 0.001$ versus the controls; $^{\dagger}P < 0.05$; $^{\dagger\dagger\dagger}P < 0.001$ versus the pCMV-CB2 group alone (n = 3). (**p**) Representative images showing the expression of fibronectin. HKC-8 cells were transfected with pCMV-CB2 (or empty vector) plasmid in the absence or presence of β-arr1 siRNA for 24 hours. The arrow indicates positive staining. Bar = 25 μm. Ctrl, control; IB, immunoblotted; IP, immunoprecipitated; siNC, control siRNA; Src, SRC proto-oncogene. To optimize viewing of this image, please see the online version of this article at www.kidney-international.org.

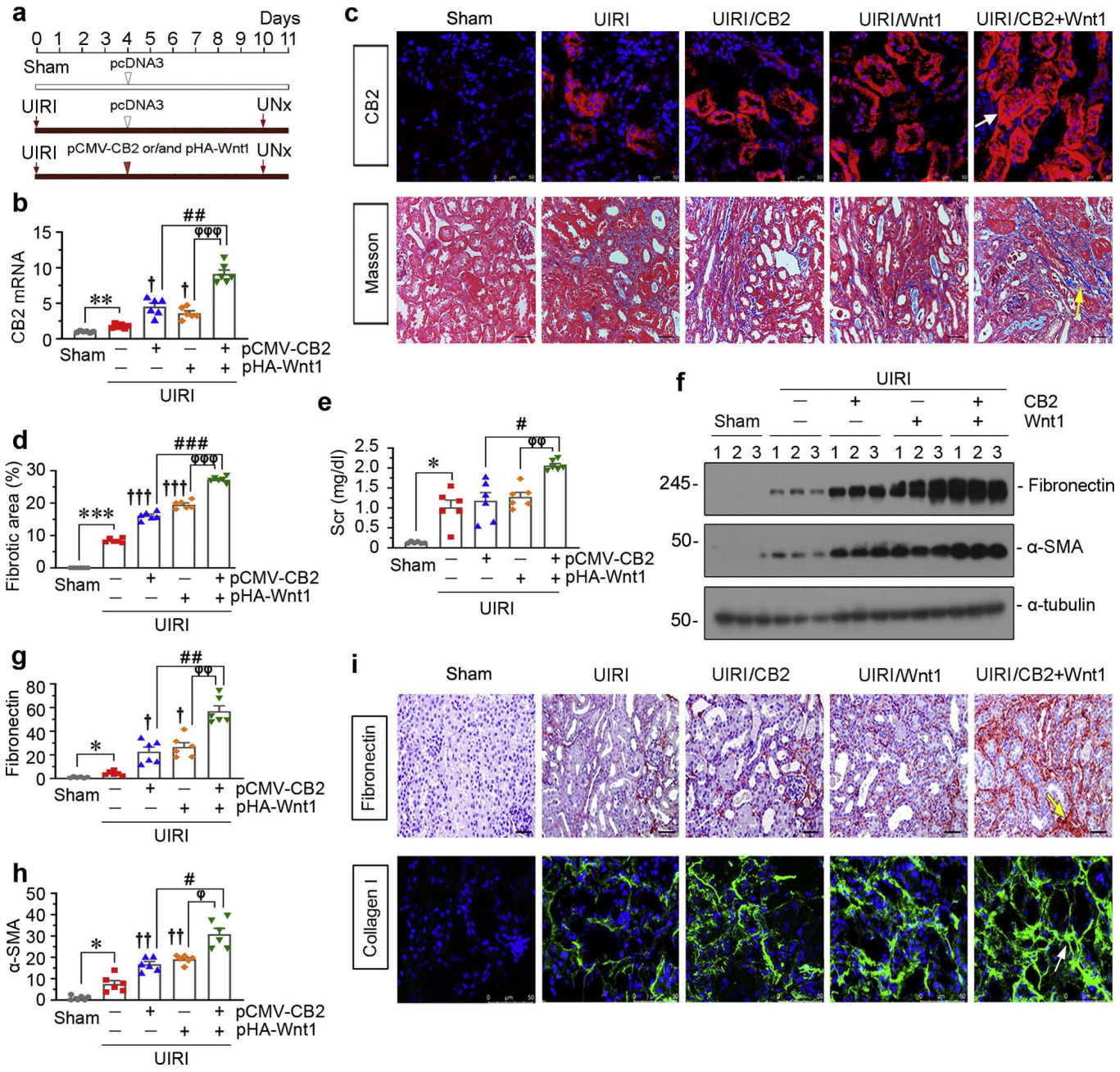

Figure 5 | Exogenous cannabinoid receptor type 2 (CB2) and Wnt1 synergistically induce renal fibrosis in unilateral ischemia-reperfusion injury (UIRI) mice. (**a**) Experimental design: Red arrows indicate the timing of renal UIRI and nephrectomy surgery. The arrowheads indicate plasmid injections of various expression vectors, including pcDNA3, pCMV-CB2, pHA-Wnt1, and a combination of pHA-Wnt1 and pCMV-CB2 at 4 days after UIRI. (**b**) Quantitative polymerase chain reaction results show renal expression of CB2 in different groups, as indicated. $^{**}P < 0.01$ versus the sham control group; $^{\dagger}P < 0.05$ versus the UIRI group alone; $^{\#\#}P < 0.01$ versus the UIRI group injected with pCMV-CB2; $^{\varphi\varphi\varphi}P < 0.001$ versus the UIRI group injected with pHA-Wnt1 (n = 6). (**c**) Representative micrographs showing CB2 and Masson's trichrome staining in different groups, as indicated. Frozen kidney sections were stained for CB2 using fluorescence *in situ* hybridization. Paraffin-embedded kidney sections were stained with Masson's trichrome staining. Arrows indicate positive staining. Bar = 50 μm. (**d**) Graphical representations of the degree of kidney fibrotic lesions in different groups after quantitative determination of Masson's staining intensity. $^{***}P < 0.001$ versus the sham control group; $^{\dagger\dagger\dagger}P < 0.001$ versus the UIRI group alone; $^{\#\#\#}P < 0.001$ versus the UIRI group injected with pCMV-CB2; $^{\varphi\varphi\varphi}P < 0.001$ versus the UIRI group injected with pHA-Wnt1 (n = 6). (**e**) Graphic presentation shows serum creatinine levels in different groups. $^{*}P < 0.05$ versus the sham control group; $^{\#}P < 0.05$ versus the UIRI group injected with pCMV-CB2; $^{\varphi\varphi}P < 0.01$ versus the UIRI group injected with pHA-Wnt1 (n = 6). (**f–h**) Representative Western blot analysis and quantitative data show the expression levels of fibronectin and α–smooth muscle actin (SMA) in different groups, as indicated. Numbers (1–3) indicate each individual animal in a given group. $^{*}P < 0.05$ versus the sham control group; $^{\dagger}P < 0.05$; $^{\dagger\dagger}P < 0.01$ versus the UIRI group alone; $^{\#}P < 0.05$; $^{\#\#}P < 0.01$ versus the UIRI group injected with pCMV-CB2; $^{\varphi}P < 0.05$; $^{\varphi\varphi}P < 0.01$ versus the the UIRI group injected with pHA-Wnt1 (n = 6). (**i**) Representative micrographs show the expression of fibronectin and collagen I in different groups. Paraffin kidney sections were immunostained with an antibody against fibronectin. Frozen kidney sections were stained with an antibody against collagen I. Arrows indicate positive staining. Bar = 50 μm. Scr, serum creatinine; UNx, unilateral nephrectomy. To optimize viewing of this image, please see the online version of this article at www.kidney-international.org.

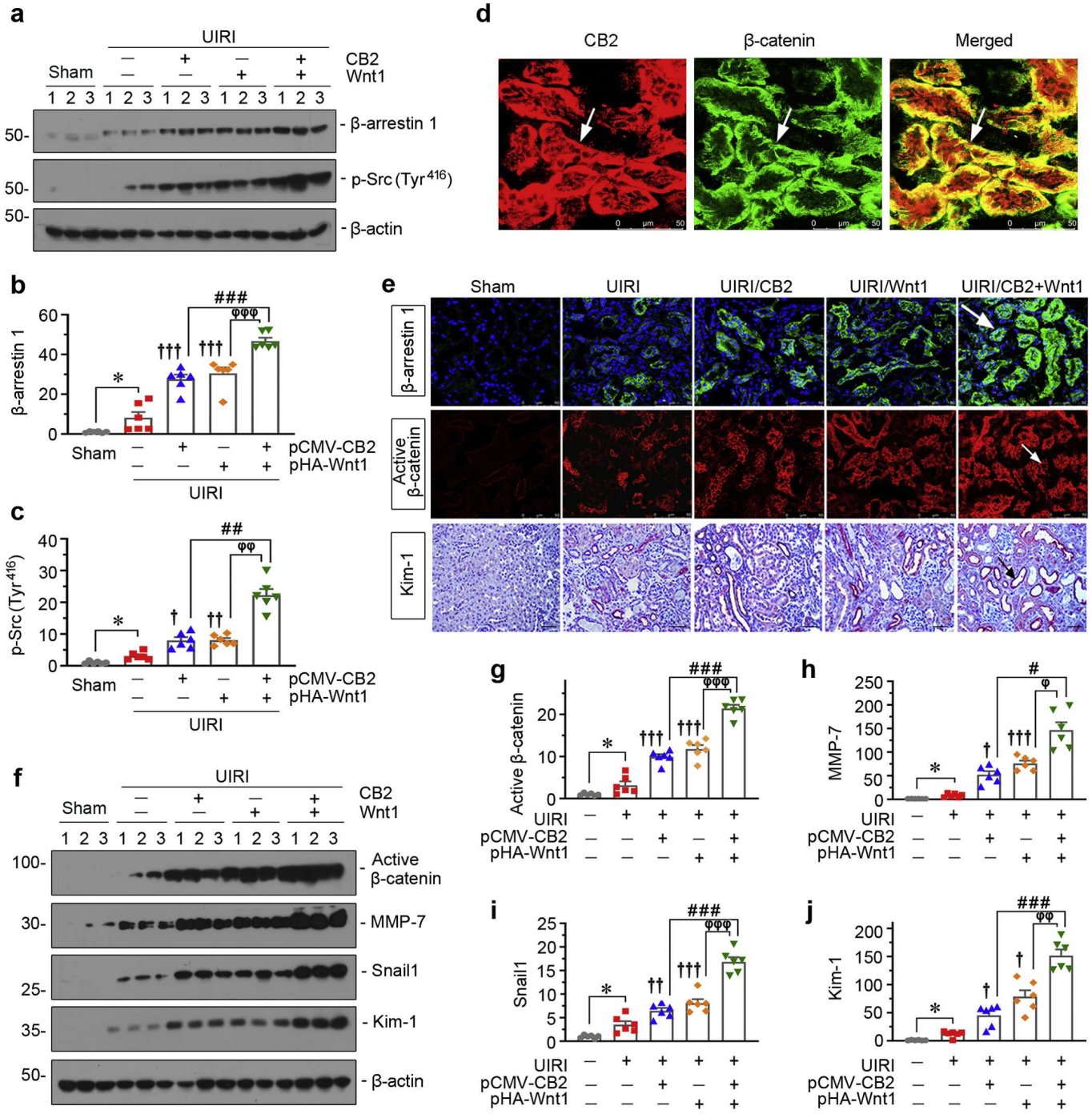

Figure 6| Cannabinoid receptor type 2 (CB2) amplifies Wnt signaling by promoting the β-arrestin 1/ SRC proto-oncogene (Src)/β-catenin pathway. (**a–c**) Representative Western blot and quantitative data showing renal expression of β-arrestin 1 and phospho (p)-Src (Tyr^{416}) in different groups. Numbers (1–3) indicate each individual animal in a given group. $^{*}P < 0.05$ versus the sham control group; $^{\dagger}P < 0.05$; $^{\dagger\dagger}P < 0.01$; $^{\dagger\dagger\dagger}P < 0.001$ versus the unilateral ischemia-reperfusion injury (UIRI) group alone; $^{\#\#}P < 0.01$; $^{\#\#\#}P < 0.001$ versus the UIRI group injected with pCMV-CB2; $^{\varphi\varphi}P < 0.01$; $^{\varphi\varphi\varphi}P < 0.001$ versus the UIRI group injected with pHA-Wnt1 (n = 6). (**d**) Representative micrographs showing the colocalization of CB2 and β-catenin in tubules of UIRI mice injected with pHA-Wnt1 and pCMV-CB2. Cryosections were subjected to fluorescence *in situ* hybridization (FISH) staining of CB2 (red) and costained with β-catenin (green) by immunofluorescence. Arrows indicate positive staining. Bar = 50 μm. (**e**) Representative micrographs show the expression of β-arrestin 1, active β-catenin, and kidney injury molecule-1 (Kim-1). Frozen kidney sections were stained with antibodies against β-arrestin 1 and active β-catenin. Paraffin kidney sections were stained with an antibody against Kim-1. Arrows indicate positive staining. Bar = 50 μm. (**f–j**) Representative Western blot and quantitative data show renal expression of active β-catenin, matrix metalloproteinase (MMP)-7, Snail1, and Kim-1. Numbers (1–3) indicate each individual animal in a given group. $^{*}P < 0.05$ versus the sham control group; $^{\dagger}P < 0.05$, $^{\dagger\dagger}P < 0.01$, $^{\dagger\dagger\dagger}P < 0.001$ versus the UIRI group alone; $^{\#}P < 0.05$; $^{\#\#\#}P < 0.001$ versus the UIRI group injected with pCMV-CB2; $^{\varphi}P < 0.05$; $^{\varphi\varphi}P < 0.01$; $^{\varphi\varphi\varphi}P < 0.001$ versus the UIRI group injected with pHA-Wnt1 (n = 6). To optimize viewing of this image, please see the online version of this article at www.kidney-international.org.

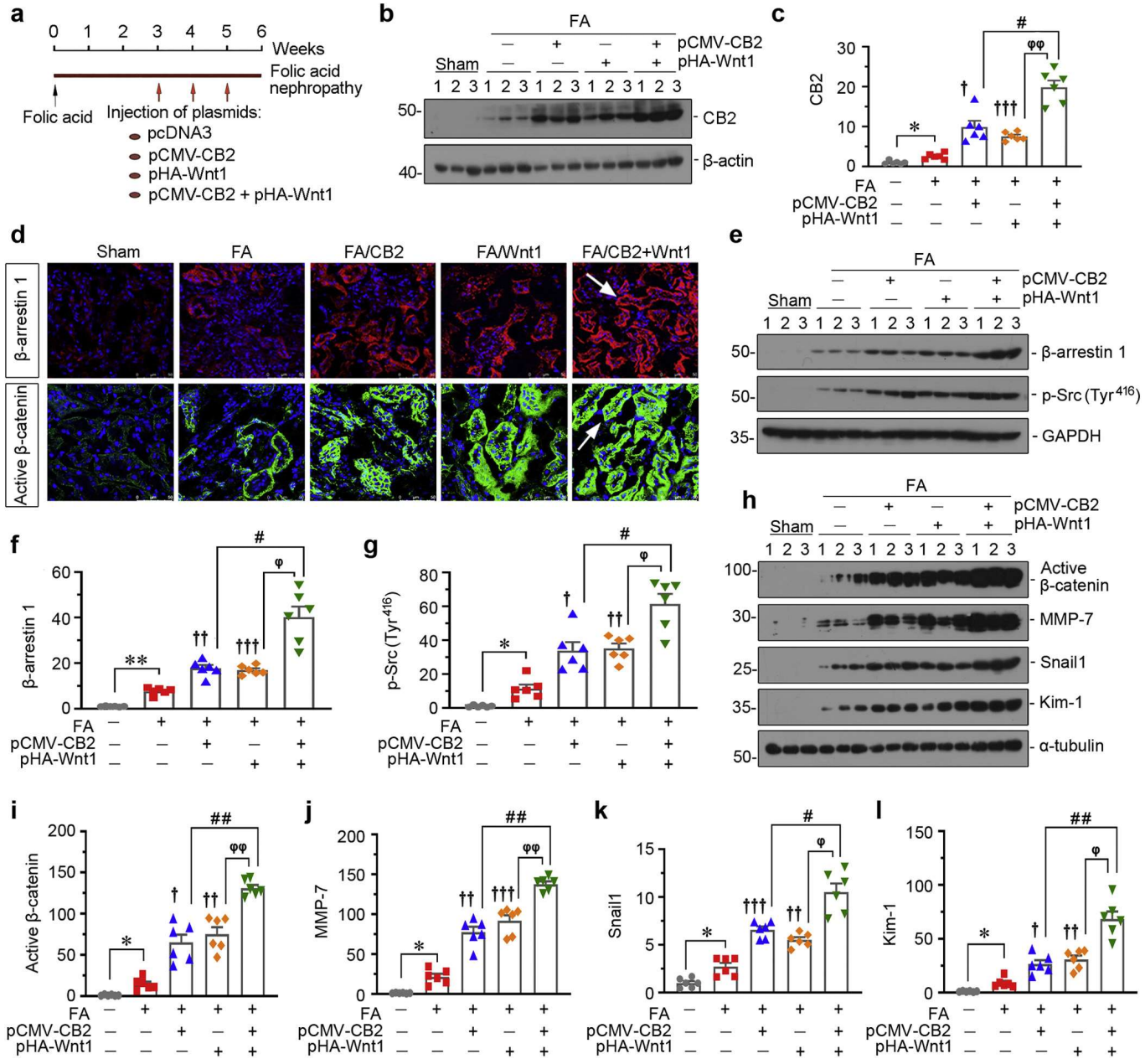

Figure 7| Exogenous cannabinoid receptor type 2 (CB2) and Wnt1 synergistically induce β-catenin signaling in folic acid–induced nephropathy. (**a**) Experimental design. Red arrows indicate injections of various expression plasmids including pcDNA3, pHA-Wnt1, pCMV-CB2, and pHA-Wnt1+pCMV-CB2 at indicated time points. Mice were intraperitoneally injected with folic acid (FA; 25 mg/kg). (**b**,**c**) Representative Western blot and quantitative data show the expression of CB2 in different groups. Numbers (1–3) indicate each individual animal in a given group. $^{*}P < 0.05$ versus the sham control group; $^{\dagger}P < 0.05$; $^{\dagger\dagger\dagger}P < 0.001$ versus the FA treatment group alone; $^{\#}P < 0.05$ versus the FA+pCMV-CB2 group alone; $^{\varphi\varphi}P < 0.01$ versus the FA+pHA-Wnt1 group alone (n = 6). (**d**) Representative micrographs show the expression of β-arrestin 1 and active β-catenin. Arrows indicate positive staining. Bar = 50 μm. (**e–g**) Representative Western blot and quantitative data show renal expression of β-arrestin 1 and phospho (p)-Src (Tyr^{416}) in different groups. Numbers (1–3) indicate each individual animal in a given group. $^{*}P < 0.05$; $^{**}P < 0.01$ versus the sham control group; $^{\dagger}P < 0.05$; $^{\dagger\dagger}P < 0.01$; $^{\dagger\dagger\dagger}P < 0.001$ versus the FA treatment group alone; $^{\#}P < 0.05$ versus the FA+pCMV-CB2 group alone; $^{\varphi}P < 0.05$ versus the FA+pHA-Wnt1 group alone (n = 6). (**h–l**) Representative Western blot and quantitative data show renal active β-catenin, matrix metalloproteinase (MMP)-7, Snail1, and kidney injury molecule-1 (Kim-1) expression in different groups. Numbers (1–3) indicate each individual animal in a given group. $^{*}P < 0.05$ versus the sham control group; $^{\dagger}P < 0.05$; $^{\dagger\dagger}P < 0.01$; $^{\dagger\dagger\dagger}P < 0.001$ versus the FA treatment group alone; $^{\#}P < 0.05$; $^{\#\#}P < 0.01$ versus the FA+pCMV-CB2 group alone; $^{\varphi}P < 0.05$; $^{\varphi\varphi}P < 0.01$ versus the FA+pHA-Wnt1 group alone (n = 6). GAPDH, glyceraldehyde 3-phosphate dehydrogenase; p-Src, phospho Src. To optimize viewing of this image, please see the online version of this article at www.kidney-international.org.

β-catenin expression plasmid.[38] Chromatin immunoprecipitation assay showed that overexpression of β-catenin promoted T-cell factor or lymphoid enhancer binding factor-1 binding to the T-cell factor/lymphoid enhancer binding factor binding sites consensus sequences of the CB2 gene promoter regions (Figure 10b) and upregulation

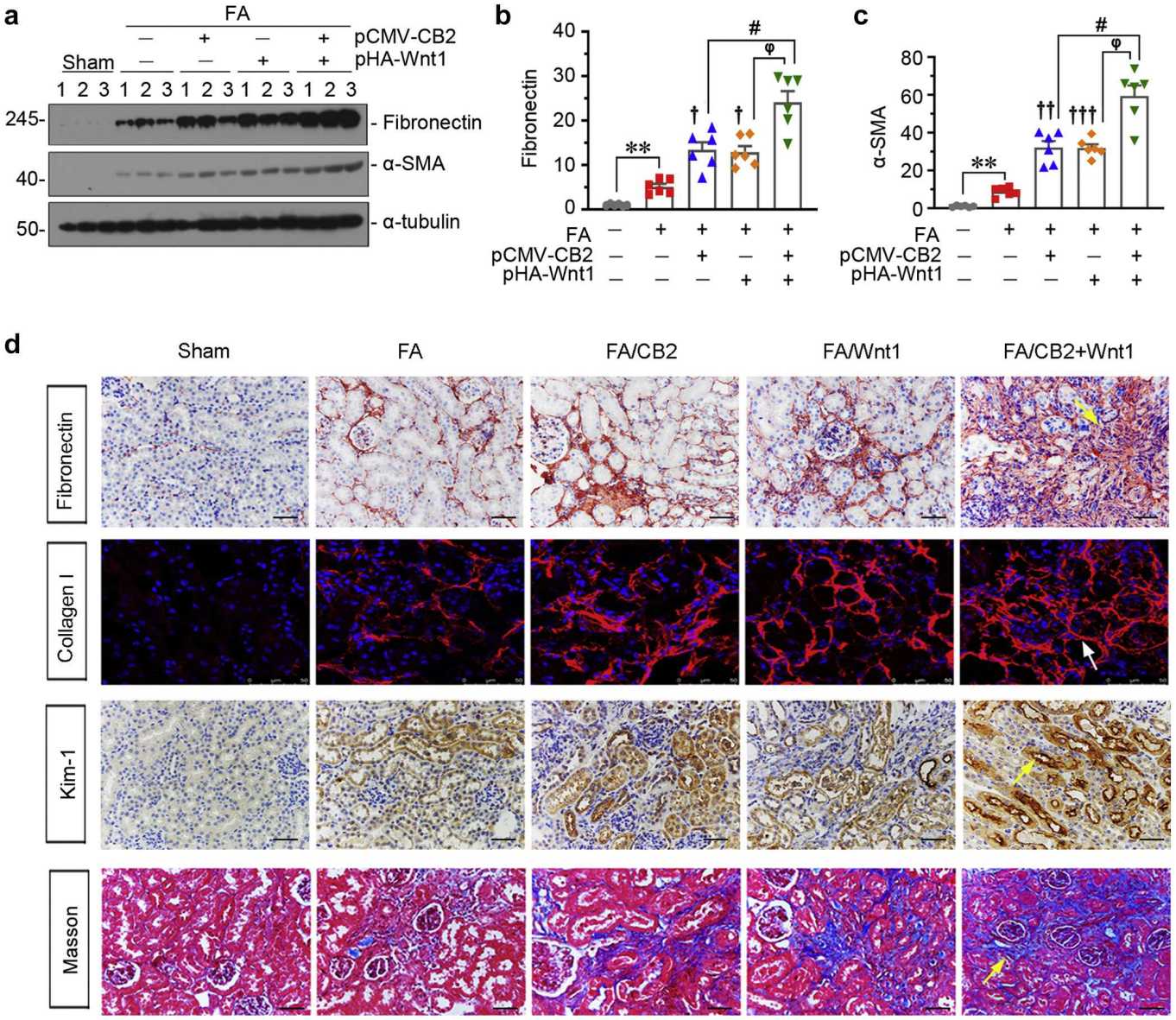

Figure 8| Exogenous cannabinoid receptor type 2 (CB2) and Wnt1 synergistically induce renal fibrosis in folic acid (FA)–induced nephropathy. (**a–c**) Representative Western blot and quantitative data show renal fibronectin and α–smooth muscle actin expression in different groups. Numbers (1–3) indicate each individual animal in a given group. $^{**}P < 0.01$ versus the sham control group; $^{\dagger}P < 0.05$; $^{\dagger\dagger}P < 0.01$; $^{\dagger\dagger\dagger}P < 0.001$ versus the FA treatment group alone; $^{\#}P < 0.05$ versus the FA+pCMV-CB2 group alone; $^{\varphi}P < 0.05$ versus the FA+pHA-Wnt1 group alone (n = 6). (**d**) Representative micrographs show renal expression of fibronectin, collagen I, kidney injury molecule-1 (Kim-1), and Masson's trichrome staining in different groups. Arrows indicate positive staining. Bar = 50 μm. To optimize viewing of this image, please see the online version of this article at www.kidney-international.org.

of CB2 mRNA (Figure 10c) and protein (Figure 10d and e), suggesting the stimulatory effects of β-catenin on CB2. Forced β-catenin further triggered the formation of a CB2/β-arrestin 1/Src complex (Figure 10f). Interference with CB2 inhibited β-catenin–induced expression of β-arrestin 1 and Src (Figure 10g–i), suggesting secondary activation of β-catenin–induced CB2 upregulation. Collectively, our results suggest that the CB2/β-catenin pathway appears to create a reciprocal activation feedback loop that plays an important role in the pathogenesis of renal fibrosis (Figure 10j).

DISCUSSION

The prevalence of CKD is increasing, and the risk for end-stage renal disease is high.[39] However, currently, there are no therapeutic drugs available.

GPCRs play fundamental roles in the fine-tuning of physiology, and they are also involved in many pathologic processes.[40–43] In kidney diseases, some GPCRs have been identified as being promising therapeutic targets.[22–24,44] Notably, β-arrestin 1 and Src serve as downstream effectors of GPCRs.[23] These signals could trigger the transactivation of β-catenin, an important contributor to kidney fibrogenesis.[38]

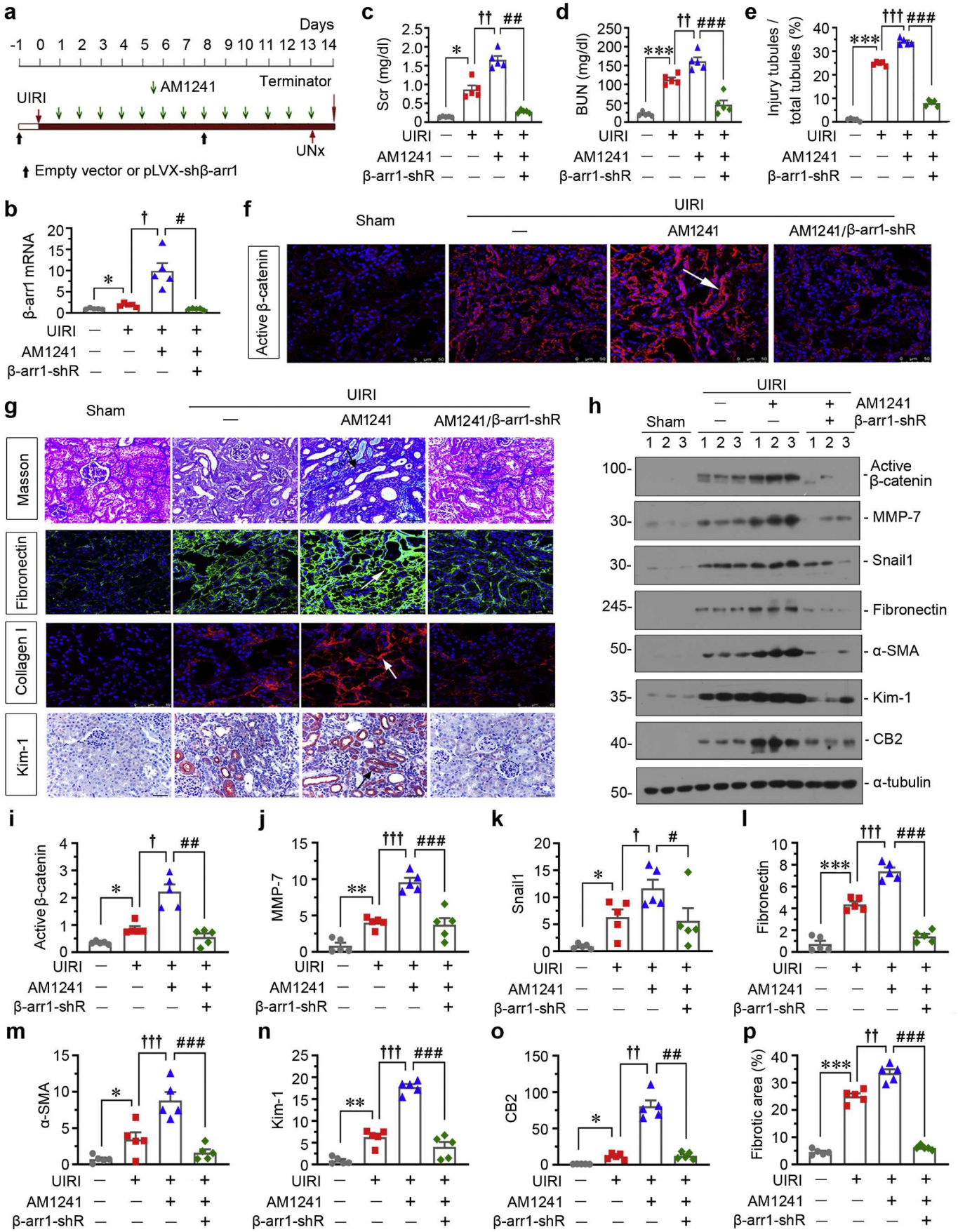

Figure 9| Knockdown of β-arrestin 1 (β-arr1) ameliorates β-catenin signaling and renal fibrosis induced by administration of aminoalkylindole (AM)1241 in unilateral ischemia-reperfusion injury (UIRI) mice. (**a**) Experimental design: Red arrows (continued)

However, it has rarely been reported that there is a relationship between CB2 and β-catenin.

CB2 is a member of the GPCR family.[5] We previously found that CB2 is expressed in tubular cells, fibroblasts, and macrophages.[11] CB2 is also expressed in podocytes and mesangial cells.[3,13] The role of CB2 in CKD was controversial in the past. Despite the upregulation of CB2 mRNA and its main endogenous ligand 2-AG in CKD models, it was previously reported that a CB2 agonist could ameliorate renal fibrosis.[7] In contrast, our previous studies identified a deleterious role of CB2 in renal fibrosis through genetic knockout experiments and assays with the more selective CB2 inverse agonist XL-001, a novel CB2 inverse agonist that exhibits the strongest binding affinity to the CB2 receptor, with the best selectivity over the CB1 receptor (2594-fold) and a Ki of 0.5 nM.[11] Of note, β-catenin and its targets are suppressed by genetic ablation or pharmacologic inhibition of CB2.[11] Given that CB2 is a member of the GPCR family, CB2 could modulate β-catenin. However, this hypothesis needs to be validated. In this study, we showed that CB2 mediates β-catenin activation through a GPCR signal wave.

Our study also confirms the emerging role of the endocannabinoid system in renal fibrosis. Of the 2 main endocannabinoids, anandamide (N-arachidonoylethanolamine) has a higher affinity for CB1, whereas 2-AG has a similar affinity for CB1 and CB2 (its affinity for CB1 is slightly higher).[45] Hence, 2-AG is the primary endocannabinoid agonist for the CB2 receptor.[46] Notably, the kidney cortex exhibits similarly high basal levels of anandamide and 2-AG[47]; however, 2-AG levels are increased more in obstructive fibrosis of the kidney, accompanied by the decrease in anandamide levels, which results in the activation of both CB2 and CB1.[7] Of note, the detrimental role of CB2 in the pathogenesis of renal fibrosis was demonstrated by genetic approaches in our recent study,[11] and is further confirmed in the present study.

Although a previous report showed that CB2 is expressed by both inflammatory cells and podocytes at a high basal level,[48] CB2 and its main endogenous ligand 2-AG are actually upregulated after UUO and IRI.[7,11] Notably, in renal fibrosis of mice and a variety of human nephropathies, CB2 is predominantly expressed in renal tubular epithelium as well as in interstitial fibroblasts and leukocytes (Figure 2; Supplementary Figure S1), suggesting that the upregulation of CB2 is a common pathologic feature in the fibrotic kidneys. In our animal studies, we adopted fluorescence *in situ* hybridization of CB2 to identify its expression pattern because of its low cost. The staining revealed that CB2 is mainly expressed in tubular epithelium. The reason behind this discrepancy may lie in the sensitivity of the fluorescence *in situ* hybridization technique in the detection of highly abundant mRNAs and the exposure time for imaging. We observed CB2 in not only the cell membrane, but also the tubular cytoplasmic area, suggesting receptor internalization into intracellular compartments, such as endosomes and lysosomes.[26,27] The specificity of the fluorescence *in situ* hybridization assay was confirmed with a primary CB2 antibody, and both were checked in CB2 knockout mice (Supplementary Figure S1). Interestingly, we observed heterodimer formation of CB2 with CB1 in UUO-affected kidneys and transforming growth factor–β-induced tubular cells (Supplementary Figure S4), suggesting that their stimulatory effects may be synergistic. However, CB1 expression was not affected by AM1241 or XL-001, which adds further complexity to the mechanisms. As previously mentioned regarding the mutually inhibitory effects of CB2 and CB1,[6] more studies should be performed to verify their interconnected effects, an investigation beyond the scope of the current study. Nevertheless, our previous and present findings consistently reveal that blockade of CB2 is a potential therapeutic intervention strategy to prevent renal fibrosis. Along with informing patients with CKD, our findings provide health warnings to the fast-growing group

Figure 9 | (continued) indicate the timing of renal IRI and nephrectomy surgery. Black arrows indicate plasmid injections of various expression vectors, including empty vector or shRNA for β-arrestin 1 plasmid (pLVX-shβ-arr1). Green arrows indicate administrations of AM1241 (10 mg/kg). (**b**) β-arr1 mRNA levels in different groups were assessed by real-time polymerase chain reaction. $^{*}P < 0.05$ versus the sham control group; $^{\dagger}P < 0.05$ versus the UIRI group alone; $^{\#}P < 0.05$ versus the UIRI group with AM1241 (n = 5). (**c**,**d**) Knockdown of β-arr1 significantly decreased serum creatinine and blood urea nitrogen (BUN) levels. $^{*}P < 0.05$; $^{***}P < 0.001$ versus the sham control group; $^{\dagger\dagger}P < 0.01$ versus the UIRI group alone; $^{\#\#}P < 0.01$; $^{\#\#\#}P < 0.001$ versus the UIRI group with AM1241 (n = 5). (**e**) Quantitative analysis of tubular injury in different groups as indicated. Kidney sections were subjected to periodic acid–Schiff staining. At least 10 randomly selected fields were evaluated under original magnification ×400, and results were averaged for each animal. $^{***}P < 0.001$ versus the sham control group; $^{\dagger\dagger\dagger}P < 0.001$ versus the UIRI group alone; $^{\#\#\#}P < 0.001$ versus the UIRI group with AM1241 (n = 5). (**f**) Representative micrographs showing active β-catenin expression in different groups. Frozen kidney sections were stained with an antibody against active β-catenin. The arrow indicates positive staining. Bar = 50 μm. (**g**) Representative micrographs showing Masson's trichrome staining and the expression of fibronectin, collagen I, and kidney injury molecule-1 (Kim-1) in different groups. Paraffin sections were subjected to Masson's trichrome staining and immunostained with an antibody against Kim-1. Cryosections were immunostained with antibodies against fibronectin and collagen I. Arrows indicate positive staining. Bar = 50 μm. (**h–o**) Representative Western blot and quantitative data show renal expression of active β-catenin, matrix metalloproteinase (MMP)-7, Snail1, fibronectin, α–smooth muscle actin (SMA), Kim-1, and cannabinoid receptor type 2 (CB2). $^{*}P < 0.05$; $^{**}P < 0.01$; $^{***}P < 0.001$ versus the sham control group; $^{\dagger}P < 0.05$; $^{\dagger\dagger}P < 0.01$; $^{\dagger\dagger\dagger}P < 0.001$ versus the UIRI group alone; $^{\#}P < 0.05$; $^{\#\#}P < 0.01$; $^{\#\#\#}P < 0.001$ versus the UIRI group with AM1241 (n = 5). (**p**) Graphical representation of kidney fibrotic lesions in different groups. $^{***}P < 0.001$ versus the sham control group; $^{\dagger\dagger}P < 0.01$ versus the UIRI group alone; $^{\#\#\#}P < 0.001$ versus the UIRI group with AM1241 (n = 5). Scr, serum creatinine; shR, shRNA control plasmid; Unx, unilateral nephrectomy. To optimize viewing of this image, please see the online version of this article at www.kidney-international.org.

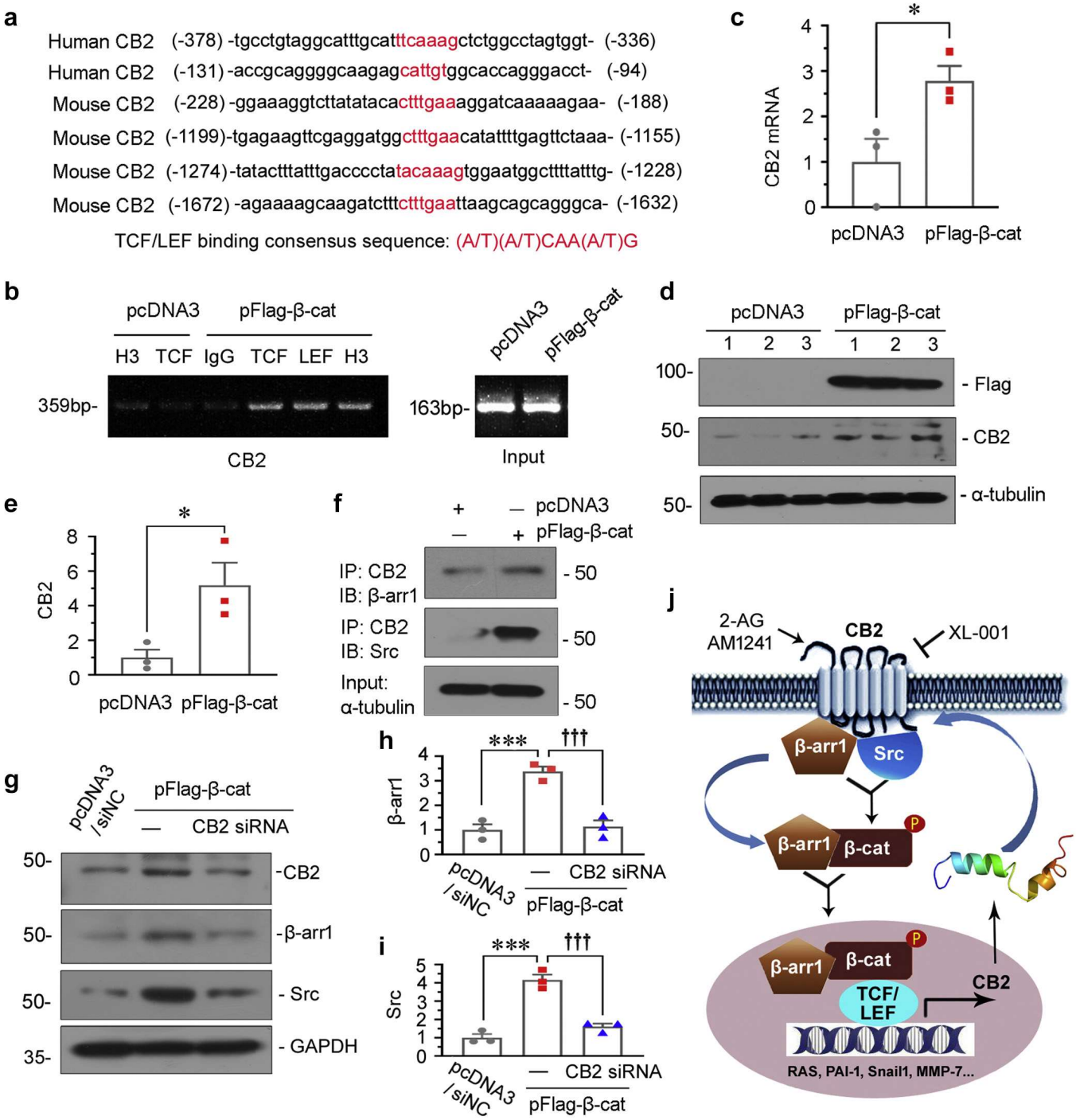

Figure 10 | Cannabinoid receptor type 2 (CB2) is a downstream target of β-catenin (β-cat). (**a**) Bioinformatics analysis revealed the presence of putative T-cell factor (TCF) binding sites (TBSs) in the promoter region of human and mouse CB2 genes. The sequences and positions of the putative TBSs in the CB2 genes are highlighted (red), whereas the TBS consensus sequence is given at the bottom of this panel. (**b**) Representative chromatin immunoprecipitation (ChIP) assay results showing the binding of TCF or lymphoid enhancer binding factor (LEF)-1 to the CB2 gene promoter region. Human kidney proximal tubular (HKC)-8 cells were transfected with β-catenin expression plasmid (pFlag-β-cat) or pcDNA3 for 24 hours. Cell lysates were precipitated with an antibody against TCF, LEF-1, histone H3, or nonimmune IgG, and the ChIP assay was performed for CB2 gene promoters. Total diluted lysate was used as total genomic input DNA. (**c**) Graphic presentation of CB2 mRNA level. HKC-8 cells were transfected with pFlag-β-cat or pcDNA3 plasmid. Total RNA was analyzed by quantitative polymerase chain reaction. $^{*}P < 0.05$ versus the pcDNA3 group (n = 3). (**d**,**e**) Representative Western blot and quantitative data show overexpression of β-catenin–induced upregulation of CB2. $^{*}P < 0.05$ versus the pcDNA3 group (n = 3). (**f**) Representative graphs show β-catenin induced the formation of a CB2/β-arrestin 1(β-arr1)/ proto-oncogene Src complex. Cell lysates were immunoprecipitated (IP) with an antibody against CB2, followed by immunoblotting (IB) with anti-β-arrestin 1 (β-arr1), or anti-Src. (**g–i**) Representative Western blot and quantitative data show the expression of CB2, β-arrestin 1 (β-arr1), and Src. HKC-8 cells were transfected with pFlag-β-cat (or pcDNA3) plasmid in the presence or absence of CB2 small interfering RNA (siRNA). $^{***}P < 0.001$ versus the pcDNA3 group; $^{\dagger\dagger\dagger}P < 0.001$ versus the pFlag-β-catenin group alone (n = 3). (Continued)

of exocannabinoid consumers, for both recreational and medicinal purposes.[49] Chronic heavy use could lead to the continuous activation of both CB1 and CB2 receptors, which may have negative effects on kidney health.

Although a previous report showed that β-arrestin 1 plays a role in renal fibrosis and activation of β-catenin,[50] we further clarify the functional mechanisms of the β-arrestin 1-mediated CB2/β-catenin pathway in detail. We found β-arrestin 1 is more abundant than β-arrestin 2 in IRI mice (data not shown). It is well known that β-arrestin 1 is responsible for GPCR activation and downstream signal transduction via Src, AKT, extracellular signal-regulated protein kinase (ERK1/2), and other kinases.[25,27,28] Given that activation of Src could mediate several pro-fibrosis pathways, such as epidermal growth factor receptor and signal transducer and activator of transcription (STAT)3,[29] we could not exclude the possibility that these pathways are also the downstream pathways of CB2. Nevertheless, our observations suggest that β-catenin signaling is mediated by CB2-induced β-arrestin 1/Src complex. In addition, β-arrestin 1 is a master checkpoint regulator, and it serves as a scaffold protein to initiate the activation of β-catenin by translocating it to the nucleus. Another novel finding is that CB2 is a target of β-catenin. Several targets of β-catenin have been previously reported by our group.[34,38] CB2 was identified in this study. Hence, it is notable that the CB2/β-catenin pathway appears to create a reciprocal activation loop that cooperatively promotes the pathogenesis of renal fibrosis.

In summary, our results suggest that aberrantly expressed CB2 is critically involved in renal fibrosis through β-arrestin 1–induced β-catenin activation. β-catenin triggers the expression of CB2, which facilitates receptor activation and transmission of the signal wave. These results (i) illustrate a novel CB2/β-catenin pathway that promotes renal fibrosis and (ii) implicate that targeted inhibition of CB2 or β-arrestin 1 may protect against fibrosis through inhibition of the reciprocal activation loop.

CONCISE METHODS

For detailed methods, see the Supplementary Methods.

Animal models

Male C57BL/6 mice were purchased from the Experimental Animal Center of Southern Medical University (Guangzhou, China). For the IRI model, bilateral pedicles were clipped by microaneurysm clamps for 32 minutes at 37.5 °C during the ischemia and recovery period. The UUO model was established by triple-ligating the left ureter with 4-0 silk after an abdominal midline incision. For the UIRI model, the left pedicles were clipped for 35 minutes using microaneurysm clamps, and the contralateral kidney was removed 1 day before sacrifice. For the folic acid–induced nephropathy model, male C57BL/6 mice were treated with folic acid via a single intraperitoneal injection of 25 mg/kg body weight. *In vivo* expression of Wnt1 or CB2 or knockdown of β-arrestin 1 in mice was carried out by a hydrodynamic-based gene delivery approach.[11,35] The detailed experimental designs are shown in Figures 5a, 7a, and 9a. The animal experiments were approved by the Animal Ethics Committee at Southern Medical University, Guangzhou, China. Breeding pairs of the CB2 null mice ($CB2^{-/-}$) aged 6–8 weeks, in C57BL/6N background, were purchased from Cyagen Biosciences (stock no. KOCMP-21582-Cnr2; Cyagen Biosciences, Guangzhou, China). CB2 receptor deficiency was confirmed by reverse transcription–PCR.

Human kidney biopsy samples and cell culture

Human kidney sections (3 μm) were obtained from renal biopsies performed at the Nanfang Hospital and the Huadu District People's Hospital, Southern Medical University, Guangzhou, China. Normal control biopsies were derived from nontumor kidney tissues of patients who had renal carcinoma. The studies involving human kidney sections were performed with informed patient consent and were approved by the Institutional Ethics Committee at Nanfang Hospital and the Huadu District People's Hospital. Human proximal tubular epithelial cells (HKC-8) were provided by Dr. Lorraine C. Racusen (Johns Hopkins University, Baltimore, MD). Nuclear and cytoplasmic fractions were separated with a commercial kit (BestBio, Shanghai, China).

Determination of serum creatinine and blood urea nitrogen levels

Serum creatinine and blood urea nitrogen levels were determined by an automatic chemistry analyzer (AU480 Chemistry Analyzer, Beckman Coulter, Atlanta, GA).

In situ hybridization

CB2 probes were purchased from Boster Technology, Wuhan, China. Kidney sections (8 μm) were fixed with 4% formaldehyde and assessed by fluorescence staining of CB2 using a commercial kit (MK2530, Boster Biological Technology, Wuhan, China).

Histology and immunohistochemical and immunofluorescence staining

Paraffin-embedded kidney sections were stained using periodic acid-Schiff and Masson's trichrome staining to identify injured tubules and determine collagen deposition. The lesions were quantified using a computer-aided technique.[37] Immunohistochemical and immunofluorescence staining were performed in paraffin and frozen sections, respectively. Antibodies are described in the Supplementary Methods.

Figure 10 | (Continued) (j) Diagram depicting the potential mechanism of CB2 action. Through the binding of the main endogenous ligand 2-arachidonoylglyceril (2-AG) or stimulation by the agonist aminoalkylindole (AM)1241, CB2 is activated, and this induces the recruitment of β-arrestin 1 and Src. The formation of a CB2/β-arrestin 1/Src complex triggers the activation of β-catenin through tyrosine phosphorylation. As a scaffold protein, β-arrestin 1 facilitates the nuclear translocation of active β-catenin, which then stimulates the expression of numerous target genes, such as the renin–angiotensin system (RAS), plasminogen activator inhibitor-1 (PAI-1), Snail1, and matrix metalloproteinase (MMP)-7 through the binding of TCF/LEF transcription factors. Importantly, CB2 is also a direct downstream target of β-catenin. Thus, the CB2/β-catenin pathway appears to create a reciprocal activation feedback loop that plays a central role in the pathogenesis of renal fibrosis. GAPDH, glyceraldehyde 3-phosphate dehydrogenase; siNC, control siRNA.

Western blot analysis and immunoprecipitation

Protein expression was analyzed by Western blot analysis. The interaction among proteins was detected by coimmunoprecipitation as previously described.[27] Primary antibodies used are described in the Supplementary Methods.

Quantitative real-time PCR

Total RNA was obtained using a TRIzol RNA isolation system (Life Technologies, Grand Island, NY). Real-time PCR was performed on an ABI PRISM 7000 Sequence Detection System (Applied Biosystems, Foster City, CA). The sequences of the primer pairs used in quantitative real-time PCR are described in the Supplementary Methods.

TOP-Flash luciferase reporter assay

293-T cells were transfected with the CB2 expression vector (pCMV-CB2), and cotransfected with β-arrestin1 expression vector (pCMV-β-arr1) or small interfering RNA. The luciferase assay was conducted using a dual luciferase assay system kit (E1910; Promega, Madison, WI).

Chromatin immunoprecipitation

Cell lysates were obtained, and the chromatin immunoprecipitation assay was performed using a commercial kit (ab500, Abcam, Cambridge, UK). The primary antibodies and primers are described in the Supplementary Methods.

Statistical analyses

All the data are expressed as mean ± standard error of the mean. Statistical analysis was carried out using SPSS 19.0 (SPSS Inc, Chicago, IL). Comparisons were made by Student *t*-test for comparison of 2 groups, or via 1-way analysis of variance followed by the Least Significant Difference or Dunnett's T3 procedure for comparison of more than 2 groups. A value of $P < 0.05$ was considered statistically significant. Bivariate correlation analysis was performed using Pearson and Spearman rank correlation analysis.

DISCLOSURE

All the authors declared no competing interests.

ACKNOWLEDGMENTS

This work was supported by National Key R&D Program of China (2020YFC2005000), National Natural Science Foundation of China grants (82070707, 91949114, 81722011, 81521003, and 81860131); National Key Research and Development Project 2019YFC2005000, and the Project of Innovation Team of Chronic Kidney Disease with Integrated Traditional Chinese and Western Medicine (2019KCXTD014); Frontier Research and Outstanding Scholar Programs of Guangzhou Regenerative Medicine and Health, Guangdong Laboratory (2018GZR110105004, 2018GZR110102004); and a Postdoctoral Science Foundation of China grant (2019M663007).

SUPPLEMENTARY MATERIAL

Supplementary File (PDF)

Supplementary Methods.

Figure S1. (**A**) Representative micrographs showing renal CB2 expression in IRI and UUO mice. Paraffin sections were immunostained with an antibody against CB2. Arrows indicate positive tubules. Arrowheads denote positive interstitial cells (fibroblasts or leukocytes). Bar = 50 μm. (**B**) Colocalization of CB2 and mannose R, a macrophage marker, is indicated by arrows. Frozen kidney sections from mice 7 days after IRI were immunostained with antibodies against CB2 and mannose R. (**C**) RT-PCR analysis showing renal CB2 expression in wild-type control mice (WT) and CB2 null mice (KO). (**D**) Representative micrographs showing renal CB2 expression in different groups. WT and KO mice were subjected to UUO or sham surgery and sacrificed at 7 days after operation. Paraffin sections were immunostained with an antibody against CB2. The arrow indicates positive staining. The arrowhead denotes positive interstitial cell (fibroblast or leukocyte). Bar = 50 μm. (**E**) Representative Western blot showing renal CB2 expression in WT and KO mice subjected to UUO surgery. The mice were sacrificed at 7 days after UUO. (**F**) Representative micrographs showing the fluorescence *in situ* hybridization (FISH) staining of CB2 in WT and KO mice. Frozen kidney sections were analyzed. No positive staining was observed. Bar = 50 μm. (**G**) Representative micrographs showing the FISH staining of CB2. Frozen kidney sections from UUO-affected WT or KO mice were subjected to FISH staining using specific CB2 probes or a scramble control probe. The arrow indicates positive staining. Bar = 50 μm.

Figure S2. (**A–F**) Quantitative data for Figure 3d. HKC-8 cells were transfected with empty vector (pcDNA3) or pCMV-CB2 plasmid for 24 hours. Cell lysates were immunoblotted with different antibodies. $^{*}P < 0.05$, $^{**}P < 0.01$, $^{***}P < 0.001$ versus the pcDNA3 group (n = 3).

Figure S3. Representative micrographs showing periodic acid–Schiff (PAS) staining in different groups as indicated. Arrows indicate injury tubules. Bar = 50 μm.

Figure S4. (**A,B**) Representative coimmunoprecipitation showing the binding of CB2 with CB1, and representative Western blot showing the expression of CB1 and CB2 in cultured tubular cells. HKC-8 cells were treated with transforming growth factor (TGF)-β1 (2 ng/mL) and/or AM1241 (10 μM) for 48 hours. HKC-8 cells were also pretreated with XL-001 (10 μM) for 1 hour, followed by the stimulation of transforming growth factor (TGF)-β1 (2 ng/mL) for 48 hours. Whole cell lysates were immunoprecipitated (IP) with an antibody against CB1 or CB2, followed by immunoblotting (IB) with an antibody against CB2 or CB1. Cell lysates were also immunoblotted with an antibody against CB1, CB2, or GAPDH. (**C**) Representative coimmunoprecipitation showing the binding of CB2 with CB1, and representative Western blot showing renal expression of CB1 and CB2 in UUO-affected kidneys. Mouse models of UUO with delayed administration of XL-001 were described previously,[11] and the archival kidney samples from these earlier studies were used for analyzing the binding of CB1 and CB2, as well as CB1 and CB2 protein expression. Whole kidney homogenates were immunoprecipitated (IP) with an antibody against CB1 or CB2, followed by immunoblotting (IB) with an antibody against CB2 or CB1. Kidney homogenate lysates were also immunoblotted with the antibodies against CB1, CB2, or GAPDH.

REFERENCES

1. Huang HC, Wang SS, Hsin IF, et al. Cannabinoid receptor 2 agonist ameliorates mesenteric angiogenesis and portosystemic collaterals in cirrhotic rats. *Hepatology*. 2012;56:248–258.
2. Schmole AC, Lundt R, Toporowski G, et al. Cannabinoid receptor 2-deficiency ameliorates disease symptoms in a mouse model with Alzheimer's disease-like pathology. *J Alzheimers Dis*. 2018;64:379–392.
3. Barutta F, Grimaldi S, Franco I, et al. Deficiency of cannabinoid receptor of type 2 worsens renal functional and structural abnormalities in streptozotocin-induced diabetic mice. *Kidney Int*. 2014;86:979–990.
4. Liu J, Godlewski G, Jourdan T, et al. Cannabinoid-1 receptor antagonism improves glycemic control and increases energy expenditure through sirtuin-1/mechanistic target of rapamycin complex 2 and 5'Adenosine monophosphate-activated protein kinase signaling. *Hepatology*. 2019;69:1535–1548.
5. Ruiz de Azua I, Lutz B. Multiple endocannabinoid-mediated mechanisms in the regulation of energy homeostasis in brain and peripheral tissues. *Cell Mol Life Sci*. 2019;76:1341–1363.

6. Barutta F, Bruno G, Mastrocola R, et al. The role of cannabinoid signaling in acute and chronic kidney diseases. *Kidney Int*. 2018;94:252–258.
7. Lecru L, Desterke C, Grassin-Delyle S, et al. Cannabinoid receptor 1 is a major mediator of renal fibrosis. *Kidney Int*. 2015;88:72–84.
8. Udi S, Hinden L, Earley B, et al. Proximal tubular cannabinoid-1 receptor regulates obesity-induced CKD. *J Am Soc Nephrol*. 2017;28:3518–3532.
9. Hinden L, Udi S, Drori A, et al. Modulation of renal GLUT2 by the cannabinoid-1 receptor: implications for the treatment of diabetic nephropathy. *J Am Soc Nephrol*. 2018;29:434–448.
10. Barutta F, Grimaldi S, Gambino R, et al. Dual therapy targeting the endocannabinoid system prevents experimental diabetic nephropathy. *Nephrol Dial Transplant*. 2017;32:1655–1665.
11. Zhou L, Zhou S, Yang P, et al. Targeted inhibition of the type 2 cannabinoid receptor is a novel approach to reduce renal fibrosis. *Kidney Int*. 2018;94:756–772.
12. Larrinaga G, Varona A, Perez I, et al. Expression of cannabinoid receptors in human kidney. *Histol Histopathol*. 2010;25:1133–1138.
13. Deutsch DG, Goligorsky MS, Schmid PC, et al. Production and physiological actions of anandamide in the vasculature of the rat kidney. *J Clin Invest*. 1997;100:1538–1546.
14. Netherland CD, Pickle TG, Bales A, Thewke DP. Cannabinoid receptor type 2 (CB2) deficiency alters atherosclerotic lesion formation in hyperlipidemic Ldlr-null mice. *Atherosclerosis*. 2010;213:102–108.
15. Deveaux V, Cadoudal T, Ichigotani Y, et al. Cannabinoid CB2 receptor potentiates obesity-associated inflammation, insulin resistance and hepatic steatosis. *PloS One*. 2009;4:e5844.
16. Pavlos NJ, Friedman PA. GPCR signaling and trafficking: the long and short of it. *Trends Endocrinol Metab*. 2017;28:213–226.
17. Lammermann T, Kastenmuller W. Concepts of GPCR-controlled navigation in the immune system. *Immunol Rev*. 2019;289:205–231.
18. Dorsam RT, Gutkind JS. G-protein-coupled receptors and cancer. *Nat Rev Cancer*. 2007;7:79–94.
19. Iyinikkel J, Murray F. GPCRs in pulmonary arterial hypertension: tipping the balance. *Br J Pharmacol*. 2018;175:3063–3079.
20. Pfleger J, Gresham K, Koch WJ. G protein-coupled receptor kinases as therapeutic targets in the heart. *Nat Rev Cardiol*. 2019;16:612–622.
21. Huang Y, Skwarek-Maruszewska A, Horre K, et al. Loss of GPR3 reduces the amyloid plaque burden and improves memory in Alzheimer's disease mouse models. *Sci Transl Med*. 2015;7:309ra164.
22. Mo H, Wu Q, Miao J, et al. C-X-C chemokine receptor type 4 plays a crucial role in mediating oxidative stress-induced podocyte injury. *Antioxid Redox Signal*. 2017;27:345–362.
23. Buelli S, Rosano L, Gagliardini E, et al. Beta-arrestin-1 drives endothelin-1-mediated podocyte activation and sustains renal injury. *J Am Soc Nephrol*. 2014;25:523–533.
24. Wang Y, Huang J, Liu X, et al. Beta-arrestin-biased AT1R stimulation promotes extracellular matrix synthesis in renal fibrosis. *Am J Physiol Renal Physiol*. 2017;313:F1–F8.
25. Ahn KH, Mahmoud MM, Shim JY, Kendall DA. Distinct roles of beta-arrestin 1 and beta-arrestin 2 in ORG27569-induced biased signaling and internalization of the cannabinoid receptor 1 (CB1). *J Biol Chem*. 2013;288:9790–9800.
26. Nogueras-Ortiz C, Yudowski GA. The multiple waves of cannabinoid 1 receptor signaling. *Mol Pharmacol*. 2016;90:620–626.
27. Nogueras-Ortiz C, Roman-Vendrell C, Mateo-Semidey GE, et al. Retromer stops beta-arrestin 1-mediated signaling from internalized cannabinoid 2 receptors. *Mol Biol Cell*. 2017;28:3554–3561.
28. Ma Z, Yu YR, Badea CT, et al. Vascular endothelial growth factor receptor 3 regulates endothelial function through beta-arrestin 1. *Circulation*. 2019;139:1629–1642.
29. Wang J, Zhuang S. Src family kinases in chronic kidney disease. *Am J Physiol Renal Physiol*. 2017;313:F721–F728.
30. Miao J, Liu J, Niu J, et al. Wnt/beta-catenin/RAS signaling mediates age-related renal fibrosis and is associated with mitochondrial dysfunction. *Aging Cell*. 2019;18:e13004.
31. Zhou L, Chen X, Lu M, et al. Wnt/beta-catenin links oxidative stress to podocyte injury and proteinuria. *Kidney Int*. 2019;95:830–845.
32. Luo C, Zhou S, Zhou Z, et al. Wnt9a promotes renal fibrosis by accelerating cellular senescence in tubular epithelial cells. *J Am Soc Nephrol*. 2018;29:1238–1256.
33. Zhou L, Liu Y. Wnt/beta-catenin signaling and renin-angiotensin system in chronic kidney disease. *Curr Opin Nephrol Hypertens*. 2016;25:100–106.
34. Zhou D, Tian Y, Sun L, et al. Matrix metalloproteinase-7 is a urinary biomarker and pathogenic mediator of kidney fibrosis. *J Am Soc Nephrol*. 2017;28:598–611.
35. Valenta T, Hausmann G, Basler K. The many faces and functions of beta-catenin. *Embo J*. 2012;31:2714–2736.
36. Xiao L, Zhou D, Tan RJ, et al. Sustained activation of Wnt/beta-Catenin signaling drives AKI to CKD progression. *J Am Soc Nephrol*. 2016;27:1727–1740.
37. Rosano L, Cianfrocca R, Tocci P, et al. Beta-arrestin-1 is a nuclear transcriptional regulator of endothelin-1-induced beta-catenin signaling. *Oncogene*. 2013;32:5066–5077.
38. Zhou L, Li Y, Hao S, et al. Multiple genes of the renin-angiotensin system are novel targets of Wnt/beta-catenin signaling. *J Am Soc Nephrol*. 2015;26:107–120.
39. Glassock RJ, Warnock DG, Delanaye P. The global burden of chronic kidney disease: estimates, variability and pitfalls. *Nat Rev Nephrol*. 2017;13:104–114.
40. Tang T, Gong T, Jiang W, Zhou R. GPCRs in NLRP3 inflammasome activation, regulation, and therapeutics. *Trends Pharmacol Sci*. 2018;39:798–811.
41. Daehn I, Casalena G, Zhang T, et al. Endothelial mitochondrial oxidative stress determines podocyte depletion in segmental glomerulosclerosis. *J Clin Invest*. 2014;124:1608–1621.
42. Zhang X, Han J, Man K, et al. CXC chemokine receptor 3 promotes steatohepatitis in mice through mediating inflammatory cytokines, macrophages and autophagy. *J Hepatol*. 2016;64:160–170.
43. Law IKM, Padua DM, Iliopoulos D, Pothoulakis C. Role of G protein-coupled receptors-microRNA interactions in gastrointestinal pathophysiology. *Am J Physiol Heart Circul Physiol*. 2017;313:G361–G372.
44. Tang J, Liu N, Tolbert E, et al. Sustained activation of EGFR triggers renal fibrogenesis after acute kidney injury. *Am J Pathol*. 2013;183:160–172.
45. Pacher P, Mechoulam R. Is lipid signaling through cannabinoid 2 receptors part of a protective system? *Prog Lipid Res*. 2011;50:193–211.
46. Dittel BN. Direct suppression of autoreactive lymphocytes in the central nervous system via the CB2 receptor. *Br J Pharmacol*. 2008;153:271–276.
47. Ritter JK, Li C, Xia M, et al. Production and actions of the anandamide metabolite prostamide E2 in the renal medulla. *J Pharmacol Exp Ther*. 2012;342:770–779.
48. Barutta F, Piscitelli F, Pinach S, et al. Protective role of cannabinoid receptor type 2 in a mouse model of diabetic nephropathy. *Diabetes*. 2011;60:2386–2396.
49. Park F, Potukuchi PK, Moradi H, Kovesdy CP. Cannabinoids and the kidney: effects in health and disease. *Am J Physiol Renal Physiol*. 2017;313:F1124–F1132.
50. Xu H, Li Q, Liu J, et al. Beta-arrestin-1 deficiency ameliorates renal interstitial fibrosis by blocking Wnt1/beta-catenin signaling in mice. *J Mol Med*. 2018;96:97–109.